# ON FINITE VOLUME DISCRETIZATION OF THE THREE-DIMENSIONAL BIOT POROELASTICITY SYSTEM IN MULTILAYER DOMAINS

#### A. NAUMOVICH<sup>1</sup>

**Abstract** — In this paper we propose a finite volume discretization for the three-dimensional Biot poroelasticity system in multilayer domains. For stability reasons, staggered grids are used. The discretization takes into account discontinuity of the coefficients across the interfaces between layers with different physical properties. Numerical experiments based on the proposed discretization showed second order convergence in the maximum norm for the primary and flux unknowns of the system. An application example is presented as well.

2000 Mathematics Subject Classification: 65M06, 74S10, 74L10, 76S05.

**Keywords:** Biot poroelasticity system, interface problems, finite volume discretization, finite difference method.

#### 1. Introduction

The Biot poroelasticity system [2,3,19] describes coupled elastic deformations and diffusive flows in a porous medium. The system was first based on the phenomenological theory of consolidation [2], and later it was rigorously rederived in terms of the homogenization theory [1]. The existence and uniqueness of the solution were analyzed in [18]. Apart from soil consolidation this system can model a number of other industrial and environmental processes of poroelastic nature.

The choice of the numerical method for the discretization of the poroelasticity system is not so obvious. Diffusion problems are mainly solved by finite volume methods, while elasticity problems are usually solved by finite element methods. The finite element methods currently dominate in solving the poroelasticity system (see, e.g., [12,15]). However, finite element solutions, as well as standard finite difference solutions of poroelasticity equations often show nonphysical oscillations on small times. A stable finite difference discretization at all t > 0 was proposed in [9]. There, as well as in the most works on poroelasticity, the case of homogeneous porous media is considered. However, soils, as well as many manufactured porous media, often have layered structures, with layers characterized by different porosity, permeability, mechanical, and other properties.

In [6, 16], the approach from [9] was further developed for a 1-D poroelasticity model with discontinuous coefficients, based on finite volume discretization (method of balance) [17]. In the present paper, we propose a finite volume discretization of a three-dimensional poroelasticity system in a multilayer domain. The finite volume approach proposed in [17]

<sup>&</sup>lt;sup>1</sup>Fraunhofer Institut Techno- und Wirtschaftsmathematik, Fraunhofer-Platz 1, D-67663 Kaiserslautern, Germany. E-mail: naumovic@itwm.fhg.de

for discretizing a scalar equation with discontinuous coefficients is not applicable to the elasticity or poroelasticity system in the multidimensional case because of the appearance of mixed derivatives. The approach we use in the present paper is based on the use of dual finite volume partitioning of the domain with respect to the flux variables. Interpolating piecewise-continuous polynomial functions, satisfying the interface conditions, are derived in each dual cell, and the fluxes are approximated by the respective derivatives of these polynomials. A similar approach was used earlier in discretizing scalar equations with discontinuous coefficients (see, e. g., [11]). There is also a certain similarity with the approach from [5], which, as well as [11], treats scalar elliptic equations.

One more advantage of using the finite volume method instead of the finite element method is the following: we assume that the interface can cross the elements (cells). Finite element methods usually work on grids that resolve interfaces, the exception is [7], where the interfaces are allowed to cross the elements. On the other hand, there is a variety of successful finite difference and finite volume approaches, where the interfaces are allowed to cross the grid cells, such as Immersed interface method, Explicit jump immersed interface method, Ghost fluid method etc. (see, e. g., [8, 13, 20] and references therein).

The structure of the method we use is as following. At the first stage, we follow the finite volume approach (method of balance) as described, for example, in [17]: we integrate the governing system of equations written in divergent form with respect to each element (control volume) of the basic grid, and, using the Gauss — Ostrogradski theorem, transform the volumetric integrals into surface integrals. Next, we use a simple cubature rule in order to approximate the surface integrals. Then, in each volume of the dual grids, we derive the interpolating, piecewise polynomial functions satisfying the interface conditions. These polynomials are considered as an approximation to the solution of our problem, and they are subsequently used to calculate the approximations to the fluxes.

The remainder of the paper is organized as follows. The Biot poroelasticity system and the interface conditions used are described in the next section. The third section is devoted to the finite volume discretization, it contains three subsections describing the introduced staggered grids and grid functions; the transformation of the governing equations into equations with respect to the fluxes; and the derivation of the interpolating polynomials in dual volumes. The fourth section presents the results of the numerical experiments. Finally, some conclusions are drawn.

# 2. Continuous problem formulation

The classical Biot model treats the consolidation of a linearly elastic porous solid in a domain  $\Omega$  with boundary  $\Gamma$ . In this paper, we restrict ourselves to the case of a parallelepiped domain  $\Omega$ . The porous medium is either fully saturated with a slightly compressible fluid or is almost fully saturated with an incompressible fluid.

The model can be written as the following system of partial differential equations:

$$-\nabla \cdot \mathbf{S} + \nabla p = 0, \quad \frac{\partial}{\partial t} \left( \phi \beta p + \nabla \cdot \mathbf{u} \right) + \nabla \cdot \mathbf{V} = f(\mathbf{x}, t), \tag{2.1}$$

where

$$\mathbf{S} = (S^{ij})_{i,j=1,2,3} = \mu \left( \nabla \mathbf{u} + (\nabla \mathbf{u})^{\top} \right) + \lambda \nabla \cdot \mathbf{u} \mathbf{I}$$
 (2.2)

is a second-order symmetric stress tensor and

$$\mathbf{V} = (V^i)_{i=1,2,3} = -\varkappa \nu^{-1} \nabla p \tag{2.3}$$

is the fluid velocity vector,  $\mathbf{u} = (u, v, w)$  is the displacement vector of the solid skeleton,  $\lambda$  and  $\mu$  are the Lamé coefficients of the porous medium, p is the pore fluid pressure,  $\phi$  is the porosity,  $\beta$  is the compressibility of the fluid,  $\varkappa$  is the permeability of the porous medium,  $\eta$  is the fluid viscosity,  $\mathbf{I}$  is a unit tensor, and  $f(\mathbf{x}, t)$  is the source term describing, e.g., the process of injection or extraction.

Certain initial and boundary conditions must supplement system (2.1). However, we do not focus on them here, but postpone their specification to the last section, where the conditions will be specified for each numerical experiment.

Further on, the coefficients of problem (2.1) may experience discontinuities across the interface  $z = \xi$ , and we assume them to be piecewise-constant:

$$\lambda(\mathbf{x}) = \begin{cases} \lambda_1, & z < \xi, \\ \lambda_2, & z > \xi, \end{cases} \quad \mu(\mathbf{x}) = \begin{cases} \mu_1, & z < \xi, \\ \mu_2, & z > \xi, \end{cases} \quad \varkappa(\mathbf{x}) = \begin{cases} \varkappa_1, & z < \xi, \\ \varkappa_2, & z > \xi, \end{cases} \quad \phi(\mathbf{x}) = \begin{cases} \phi_1, & z < \xi, \\ \phi_2, & z > \xi. \end{cases}$$

Larger number of interfaces can also be considered, we restrict the considerations here to just one interface only for simplicity of the presentation.

At the interface between the two media certain interface conditions linking the solutions in the two subdomains should be imposed to complete the model.

Under the assumption that despite the deformation and movement of the interface no solid mass is transported across it, we conclude that there is no jump in the normal component of the displacement of the porous skeleton, which means

$$[w] = 0. (2.4)$$

We assume also that the subdomains do not slip with respect to each other, which means that at the interface the displacements of the porous skeleton in the directions tangential to the interface are the same in the both porous subdomains, which corresponds to the conditions

$$[u] = 0, \quad [v] = 0.$$
 (2.5)

Mass conservation of the fluid phase across the interface requires the continuity condition

$$[\mathbf{V} \cdot \mathbf{n}] = 0, \tag{2.6}$$

which is the continuity of the normal component of the fluid flux relative to the porous skeleton. Since the deformation in the porous medium is not produced by the stress in the porous skeleton alone, but by the fluid pressure as well, the stress conservation across the interface should be written for the porous medium as a whole in the form

$$[(\mathbf{S} - p\mathbf{I}) \cdot \mathbf{n}] = 0. \tag{2.7}$$

We will also assume that the fluid pressure p is continuous across the interface

$$[p] = 0, (2.8)$$

which reduces (2.7) to the condition

$$[\mathbf{S} \cdot \mathbf{n}] = 0. \tag{2.9}$$

Summarizing conditions (2.4)-(2.6), (2.8), (2.9), we obtain the following continuity conditions at the interface  $\xi$ :

$$[\mathbf{u}] = 0, \quad [p] = 0, \quad [\mathbf{S} \cdot \mathbf{n}] = 0, \quad [\mathbf{V} \cdot \mathbf{n}] = 0,$$
 (2.10)

which is the continuity of the displacement, fluid pressure, normal component of the stress tensor of the porous skeleton, and normal fluid flux (see, e.g., [3, sec. 2.7.3; 4, 10]). In the formulae above **n** stands for the unit normal to the interface, and  $[q] = q|_{z=\xi+0} - q|_{z=\xi-0}$ .

Model (2.1), (2.10) can be rewritten as a system of PDEs with respect to the unknown displacement components u, v, w and the fluid pressure p. The nondimensional version of this system can be written as follows:

$$-((\lambda + 2\mu)u_x + \lambda (v_y + w_z))_x - (\mu (u_y + v_x))_y - (\mu (u_z + w_x))_z + p_x = 0,$$

$$-(\mu (v_x + u_y))_x - ((\lambda + 2\mu)v_y + \lambda (w_z + u_x))_y - (\mu (v_z + w_y))_z + p_y = 0,$$

$$-(\mu (w_x + u_z))_x - (\mu (w_y + v_z))_y - ((\lambda + 2\mu)w_z + \lambda (u_x + v_y))_z + p_z = 0,$$

$$(ap + u_x + v_y + w_z)_t - (\varkappa p_x)_x - (\varkappa p_y)_y - (\varkappa p_z)_z = f(\mathbf{x}, t), \quad (\mathbf{x}, t) \in \Omega \times (0; T], \quad (2.11)$$

$$[u] = 0, \quad [v] = 0, \quad [w] = 0, \quad [\mu (w_x + u_z)] = 0, \quad [\mu (w_y + v_z)] = 0,$$

$$[(\lambda + 2\mu)w_z + \lambda (u_x + v_y)] = 0, \quad [\varkappa p_z] = 0, \quad (\mathbf{x}, t) \in \Omega \cap (z = \xi) \times (0, T], \quad (2.12)$$

where scaling has been taken with respect to the characteristic length of the porous medium l, and some reference values  $\lambda_0$ ,  $\mu_0$ ,  $\varkappa_0$ ,  $\eta_0$ ,  $a_0$  in the formulae

$$x := \frac{x}{l}, \quad y := \frac{y}{l}, \quad z := \frac{z}{l}, \quad t := \frac{(\lambda_0 + 2\mu_0)\varkappa_0 t}{l^2\eta_0}, \quad u := \frac{u}{l}, \quad v := \frac{v}{l}, \quad w := \frac{w}{l},$$

$$p := \frac{p}{\lambda_0 + 2\mu_0}, \quad \lambda := \frac{\lambda}{\lambda_0 + 2\mu_0}, \quad \mu := \frac{\mu}{\lambda_0 + 2\mu_0}, \quad \varkappa := \frac{\varkappa/\eta}{\varkappa_0/\eta_0}, \quad f := \frac{l^2 f \eta_0}{(\lambda_0 + 2\mu_0)\varkappa_0},$$

$$a = \phi \beta(\lambda_0 + 2\mu_0) \text{ is a new nondimensional parameter.}$$

### 3. Finite volume discretization

**3.1. Staggered grids and grid notations.** To overcome stability difficulties that often arise when the discretization of the Biot model is done on collocated grids, the use of staggered grids was proposed in [21]. The pressure points of this grid are located on the physical boundary, and the displacement points are defined at the respective cell faces. In the three-dimensional case, a staggered grid is composed of the following four types of grid points:

$$G^{u} = \{(x_{i+0.5}, y_{j}, z_{k}) = ((i+0.5)h_{x}, jh_{y}, kh_{z}), i = 0, \dots, N_{1} - 1, j = 0, \dots, N_{2}, k = 0, \dots, N_{3}\},$$

$$G^{v} = \{(x_{i}, y_{j+0.5}, z_{k}) = (ih_{x}, (j+0.5)h_{y}, kh_{z}), i = 0, \dots, N_{1}, j = 0, \dots, N_{2} - 1, k = 0, \dots, N_{3}\},$$

$$G^{w} = \{(x_{i}, y_{j}, z_{k+0.5}) = (ih_{x}, jh_{y}, (k+0.5)h_{z}), i = 0, \dots, N_{1}, j = 0, \dots, N_{2}, k = 0, \dots, N_{3} - 1\},$$

$$G^{p} = \{(x_{i}, y_{j}, z_{k}) = (ih_{x}, jh_{y}, kh_{z}), i = 0, \dots, N_{1}, j = 0, \dots, N_{2}, k = 0, \dots, N_{3}\}.$$

For the time discretization we introduce a grid in time with a step-size  $\tau$ 

$$G^t = \{t_n : t_n = n\tau, n = 0, 1, \dots, M\}.$$

We introduce also the following grid functions:

$$u = u_{i+0.5,j,k}^n = u_{i+0.5,j,k} = u(x_{i+0.5}, y_j, z_k, t_n), \quad v = v_{i,j+0.5,k}^n = v_{i,j+0.5,k} = v(x_i, y_{j+0.5}, z_k, t_n),$$

$$w = w_{i,j,k+0.5}^n = w_{i,j,k+0.5} = w(x_i, y_j, z_{k+0.5}, t_n), \quad p = p_{i,j,k}^n = p_{i,j,k} = p(x_i, y_j, z_k, t_n),$$

which are defined on the grids  $G^u \times G^t$ ,  $G^v \times G^t$ ,  $G^w \times G^t$ , and  $G^p \times G^t$ , respectively. The components of the discrete fluid flux and the discrete stress tensor are also defined at the appropriate grid points

$$\begin{split} V^1 &= V_{i+0.5,j,k}^{1,n} = V_{i+0.5,j,k}^1 = V^1 \big( x_{i+0.5}, y_{j}, z_{k}, t_{n} \big), \quad V^2 &= V_{i,j+0.5,k}^{2,n} = V_{i,j+0.5,k}^2 = V^2 \big( x_{i}, y_{j+0.5}, z_{k}, t_{n} \big), \\ V^3 &= V_{i,j,k+0.5}^{3,n} = V_{i,j,k+0.5}^3 = V^3 \big( x_{i}, y_{j}, z_{k+0.5}, t_{n} \big), \\ S^{11} &= S_{i,j,k}^{11,n} = S_{i,j,k}^{11} = S^{11} \big( x_{i}, y_{j}, z_{k}, t_{n} \big), \quad S^{22} = S_{i,j,k}^{22,n} = S_{i,j,k}^{22} = S^{22} \big( x_{i}, y_{j}, z_{k}, t_{n} \big), \\ S^{33} &= S_{i,j,k}^{33,n} = S_{i,j,k}^{33} = S^{33} \big( x_{i}, y_{j}, z_{k}, t_{n} \big), \\ S^{12} &= S_{i+0.5,j+0.5,k}^{12,n} = S_{i+0.5,j+0.5,k}^{12} = S^{12} \big( x_{i+0.5}, y_{j+0.5}, z_{k}, t_{n} \big), \\ S^{13} &= S_{i+0.5,j,k+0.5}^{13,n} = S_{i+0.5,j,k+0.5}^{13} = S^{13} \big( x_{i+0.5}, y_{j}, z_{k+0.5}, t_{n} \big), \\ S^{23} &= S_{i,j+0.5,k+0.5}^{23,n} = S_{i,j+0.5,k+0.5}^{23} = S^{23} \big( x_{i}, y_{j+0.5}, z_{k+0.5}, t_{n} \big). \end{split}$$

We shall use the standard notations for the finite differences on a uniform mesh (see, e.g., [17]):

$$p_x := p_{x,i,j,k} = (p_{i+1,j,k} - p_{i,j,k})/h_x, \quad p_{\bar{x}} := p_{\bar{x},i,j,k} = (p_{i,j,k} - p_{i-1,j,k})/h_x,$$

$$u_x := u_{x,i+0.5,j,k} = (u_{i+1.5,j,k} - u_{i+0.5,j,k})/h_x, \quad u_{\bar{x}} := u_{\bar{x},i+0.5,j,k} = (u_{i+0.5,j,k} - u_{i-0.5,j,k})/h_x,$$

$$u_{xy} := u_{xy,i+0.5,j,k} = (u_{i+1.5,j+1,k} - u_{i+1.5,j,k} - u_{i+0.5,j+1,k} + u_{i+0.5,j,k})/h_x h_y.$$

The finite differences  $p_y$ ,  $p_{\bar{y}}$ ,  $p_z$ ,  $p_{\bar{z}}$ ,  $u_y$ ,  $u_{\bar{y}}$ ,  $u_z$ ,  $u_{\bar{z}}$ ,  $v_x$ ,  $v_{\bar{x}}$ , etc. are defined in a similar way. We introduce the finite difference in time  $p_t = (p^{n+1} - p^n)/\tau$ , and will also use the notation

$$p^{\sigma} := \sigma p^{n+1} + (1 - \sigma)p^{n}. \tag{3.1}$$

Weighted discretization in time, as applied to the second equation of (2.1), results in the following semi-discrete equation:

$$(ap + \nabla \cdot u)_t - \nabla \cdot V^{\sigma} = f^{\sigma}, \tag{3.2}$$

where  $\sigma$  is the so-called weight parameter. This discretization corresponds to the Crank — Nicolson discretization, if  $\sigma = 0.5$  and to the fully implicit discretization if  $\sigma = 1$ , etc.

**3.2. Integral form of the governing equations.** Following the finite volume method, we integrate the first equation of (2.1) and equation (3.2) with respect to the corresponding set of the control volumes

$$\mathbf{V}^{u} = \mathbf{V}_{ijk}^{u} = (x_{i}, x_{i+1}) \times (y_{j-0.5}, y_{j+0.5}) \times (z_{k-0.5}, z_{k+0.5}),$$

$$\mathbf{V}^{v} = \mathbf{V}_{ijk}^{v} = (x_{i-0.5}, x_{i+0.5}) \times (y_{j}, y_{j+1}) \times (z_{k-0.5}, z_{k+0.5}),$$

$$\mathbf{V}^{w} = \mathbf{V}_{ijk}^{w} = (x_{i-0.5}, x_{i+0.5}) \times (y_{j-0.5}, y_{j+0.5}) \times (z_{k}, z_{k+1}),$$

$$\mathbf{V}^{p} = \mathbf{V}_{ijk}^{p} = (x_{i-0.5}, x_{i+0.5}) \times (y_{j-0.5}, y_{j+0.5}) \times (z_{k-0.5}, z_{k+0.5}).$$

Applying then the divergence theorem to the integrated equations and taking into account the interface conditions (2.10), we transform the volume integrals into surface integrals and obtain the following system of integral equations:

$$-\int_{\partial \mathbf{V}^{\mathbf{u}}} \mathbf{S}^{1} \cdot \mathbf{n}^{u} dS + \int_{\partial \mathbf{V}^{\mathbf{u}}_{\mathbf{x}}} p \cdot n_{x}^{u} dS = 0, \tag{3.3}$$

$$-\int_{\partial \mathbf{V}^{\mathbf{v}}} \mathbf{S}^{2} \cdot \mathbf{n}^{v} dS + \int_{\partial \mathbf{V}^{\mathbf{v}}} p \cdot n_{y}^{v} dS = 0, \tag{3.4}$$

$$-\int_{\partial \mathbf{V}^{\mathbf{w}}} \mathbf{S}^{3} \cdot \mathbf{n}^{w} dS + \int_{\partial \mathbf{V}^{\mathbf{w}}} p \cdot n_{z}^{w} dS = 0, \tag{3.5}$$

$$\left(\int_{\mathbf{V}^{\mathbf{p}}} ap \, dV + \int_{\partial \mathbf{V}^{\mathbf{p}}} \mathbf{u} \cdot \mathbf{n}^{p} \, dS - \tau \sigma \int_{\partial \mathbf{V}^{\mathbf{p}}} \mathbf{V} \cdot \mathbf{n}^{p} \, dS\right)^{n+1} = 
\tau \int_{\mathbf{V}^{\mathbf{p}}} f^{\sigma} \, dV + \left(\int_{\mathbf{V}^{\mathbf{p}}} ap \, dV + \int_{\partial \mathbf{V}^{\mathbf{p}}} \mathbf{u} \cdot \mathbf{n}^{p} \, dS - \tau (1 - \sigma) \int_{\partial \mathbf{V}^{\mathbf{p}}} \mathbf{V} \cdot \mathbf{n}^{p} \, dS\right)^{n}, \tag{3.6}$$

where  $\mathbf{S}^1 = (S^{11}, S^{12}, S^{13})$ ,  $\mathbf{S}^2 = (S^{12}, S^{22}, S^{23})$ ,  $\mathbf{S}^3 = (S^{13}, S^{23}, S^{33})$  are components of the stress tensor;  $\mathbf{n}^u = (n_x^u, n_y^u, n_z^u)$ ,  $\mathbf{n}^v = (n_x^v, n_y^v, n_z^v)$ ,  $\mathbf{n}^w = (n_x^w, n_y^w, n_z^w)$ ,  $\mathbf{n}^p = (n_x^p, n_y^p, n_z^p)$  are unit outward normal vectors to the volume boundaries  $\partial \mathbf{V}^{\mathbf{u}}$ ,  $\partial \mathbf{V}^{\mathbf{v}}$ ,  $\partial \mathbf{V}^{\mathbf{v}}$  and  $\partial \mathbf{V}^{\mathbf{v}}$  respectively. Control volumes' faces  $\partial \mathbf{V}^{\mathbf{u}}_{\mathbf{x}}$ ,  $\partial \mathbf{V}^{\mathbf{v}}_{\mathbf{y}}$  and  $\partial \mathbf{V}^{\mathbf{v}}_{\mathbf{z}}$  are defined by the formulae  $\partial \mathbf{V}^u_x = \partial \mathbf{V}^u \cap (\{x = x_i\} \cup \{x = x_{i+1}\})$ ,  $\partial \mathbf{V}^v_y = \partial \mathbf{V}^v \cap (\{y = y_j\} \cup \{y = y_{j+1}\})$ ,  $\partial \mathbf{V}^w_z = \partial \mathbf{V}^w \cap (\{z = z_k\} \cup \{z = z_{k+1}\})$ .

Next, we approximate the integrals over the volumes' faces in (3.3) - (3.6) by the midpoint rule and divide each equation by  $h_x h_y h_z$ , which results in the following system of discrete equations:

$$-\frac{S_{i+1,j,k}^{11} - S_{i,j,k}^{11}}{h_x} - \frac{S_{i+0.5,j+0.5,k}^{12} - S_{i+0.5,j-0.5,k}^{12}}{h_y} - \frac{S_{i+0.5,j+0.5,k}^{13} - S_{i+0.5,j,k+0.5}^{13} - S_{i+0.5,j,k-0.5}^{13}}{h_z} + \frac{p_{i+1,j,k} - p_{i,j,k}}{h_x} = 0,$$

$$-\frac{S_{i+0.5,j+0.5,k}^{12} - S_{i-0.5,j+0.5,k}^{12}}{h_x} - \frac{S_{i,j+1,k}^{22} - S_{i,j,k}^{22}}{h_y} - \frac{S_{i,j+0.5,k+0.5}^{23} - S_{i,j+0.5,k+0.5}^{23}}{h_z} + \frac{p_{i,j+1,k} - p_{i,j,k}}{h_y} = 0,$$

$$-\frac{S_{i+0.5,j,k+0.5}^{13} - S_{i-0.5,j,k+0.5}^{13}}{h_x} - \frac{S_{i,j+0.5,k+0.5}^{23} - S_{i,j-0.5,k+0.5}^{23}}{h_y} - \frac{S_{i,j,k+1}^{33} - S_{i,j,k}^{33}}{h_z} + \frac{p_{i,j,k+1} - p_{i,j,k}}{h_z} = 0,$$

$$-\frac{S_{i+0.5,j,k+0.5}^{13} - S_{i-0.5,j,k+0.5}^{13}}{h_x} - \frac{S_{i,j+0.5,k+0.5}^{23} - S_{i,j-0.5,k+0.5}^{23}}{h_y} - \frac{S_{i,j,k+1}^{33} - S_{i,j,k}^{33}}{h_z} + \frac{p_{i,j,k+1} - p_{i,j,k}}{h_z} = 0,$$

$$-\frac{S_{i+0.5,j,k+0.5}^{13} - S_{i,j,k+0.5}^{13}}{h_x} + \frac{p_{i,j,k+1} - p_{i,j,k}}{h_z} + \frac{p_{i,j,k+1} - p_{i,j,k}}{h_z} = 0,$$

$$-\frac{S_{i+0.5,j,k+0.5}^{13} - S_{i,j,k+0.5}^{13}}{h_z} + \frac{p_{i,j,k+1} - p_{i,j,k}}{h_z} = 0,$$

$$-\frac{S_{i+0.5,j,k+0.5}^{13} - S_{i,j,k+0.5}^{13}}{h_z} + \frac{p_{i,j,k+1} - p_{i,j,k}}{h_z} = 0,$$

$$-\frac{S_{i+0.5,j,k+0.5}^{13} - S_{i,j,k+0.5}^{13}}{h_z} + \frac{p_{i,j,k+1} - p_{i,j,k}}{h_z} = 0,$$

$$-\frac{S_{i+0.5,j,k+0.5}^{13} - S_{i,j,k+0.5}^{13}}{h_z} + \frac{p_{i,j,k+1} - p_{i,j,k}}{h_z} = 0,$$

$$-\frac{S_{i+0.5,j,k+0.5}^{13} - S_{i,j,k+0.5}^{13}}{h_z} + \frac{p_{i,j,k+1} - p_{i,j,k}}{h_z} = 0,$$

$$-\frac{S_{i+0.5,j,k+0.5}^{13} - S_{i,j,k+0.5}^{13}}{h_z} + \frac{p_{i,j,k+0.5}^{13} - S_{i,j,k+0.5}^{13}}{h_z} + \frac{p_{i,j,k+1}^{13} - S_{i,j,k}}{h_z} = 0,$$

$$-\frac{S_{i+0.5,j,k+0.5}^{13} - S_{i,j,k+0.5}^{13}}{h_z} + \frac{P_{i,j,k+0.5}^{13} - S_{i,j,k+0.5}^{13}}{h_z} + \frac{P_{i,j,k+0.5}^{$$

where

$$\langle a \rangle = \frac{1}{h_x h_y h_z} \int_{\mathbf{YP}} a(\mathbf{x}) \, dV, \quad \langle f \rangle = \frac{1}{h_x h_y h_z} \int_{\mathbf{YP}} f(\mathbf{x}, t) \, dV.$$
 (3.8)

**3.3. Polynomial approximation on the dual grid.** Next, we approximate the fluxes of the problem (i.e., the stress tensor and the fluid velocity vector) and transform system

(3.7) into a system of initial variables (i.e., p, u, v, w) only. For this purpose, we construct interpolating polynomials  $P(\mathbf{x})$ ,  $U(\mathbf{x})$ ,  $V(\mathbf{x})$ ,  $W(\mathbf{x})$  in the appropriately chosen sets of control volumes and then approximate the fluxes of the initial problem by the fluxes calculated on these polynomials.

Suppose that the index  $k_{\text{int}}$ ,  $0 \leq k_{\text{int}} < N_3$  is such that interface position is represented in the following way:

$$\xi = z_{k_{\text{int}}} + \theta h_z = k_{\text{int}} h_z + \theta h_z, \tag{3.9}$$

where the parameter  $0 \leq \theta < 1$ . This representation will be used below in deriving the polynomials.

First, we construct polynomials  $P(\mathbf{x})$  for the pressure unknown in each volume

$$\mathbf{V}_{i,j,k}^{P(\mathbf{x})} = \mathbf{V}^{P(\mathbf{x})} = (x_i, x_{i+1}) \times (y_j, y_{j+1}) \times (z_k, z_{k+1})$$

of the domain  $\Omega$ . Note that the volume  $\mathbf{V}_{i,j,k}^{P(\mathbf{x})}$  differs from the volume  $\mathbf{V}_{i,j,k}^p$  defined above. The approximations of the fluid flux components are calculated at the respective grid points according to the following formulae:

$$V_{i+0.5,j,k}^{1} = -\varkappa \frac{\partial P}{\partial x}(\mathbf{x}_{i+0.5,j,k}), \quad V_{i,j+0.5,k}^{2} = -\varkappa \frac{\partial P}{\partial y}(\mathbf{x}_{i,j+0.5,k}), \quad V_{i,j,k+0.5}^{3} = -\varkappa \frac{\partial P}{\partial z}(\mathbf{x}_{i,j,k+0.5}).$$

$$(3.10)$$

We prescribe polynomials  $P(\mathbf{x})$  to be piecewise-trilinear in each volume intersected by the interface  $z=\xi$  and trilinear in the other volumes. In fact, these are the highest order polynomials belonging to the kernel of the diffusion operator. The interface intersects the volume  $\mathbf{V}_{i,j,k}^{P(\mathbf{x})}$  in the case where the index k is such that  $z_k < \xi < z_{k+1}$ , which is equivalent to  $k = k_{\text{int}}$  (see representation (3.9)). The expression for such polynomials can be written as follows:

$$P(x,y,z) = \begin{cases} a_1^p(x-x_i)(y-y_j)(z-z_{k_{\text{int}}}) + b_1^p(x-x_i)(y-y_j) + \\ c_1^p(x-x_i)(z-z_{k_{\text{int}}}) + d_1^p(y-y_j)(z-z_{k_{\text{int}}}) + \\ e_1^p(x-x_i) + f_1^p(y-y_j) + g_1^p(z-z_{k_{\text{int}}}) + p_{i,j,k_{\text{int}}}, & z_{k_{\text{int}}} < z \leqslant \xi, \\ a_2^p(x-x_i)(y-y_j)(z-z_{k_{\text{int}}}) + b_2^p(x-x_i)(y-y_j) + \\ c_2^p(x-x_i)(z-z_{k_{\text{int}}}) + d_2^p(y-y_j)(z-z_{k_{\text{int}}}) + \\ e_2^p(x-x_i) + f_2^p(y-y_j) + g_2^p(z-z_{k_{\text{int}}}) + p_{i,j,k_{\text{int}}+1}, & \xi < z < z_{k_{\text{int}}+1}. \end{cases}$$
(3.11)

The unknown coefficients  $a_1^p, a_2^p, b_1^p, b_2^p, c_1^p, c_2^p, d_1^p, d_2^p, e_1^p, e_2^p, f_1^p, f_2^p, g_1^p, g_2^p$  of the polynomial can be found from the following conditions that should be fulfilled:

1) interpolation at the vertices of the volume:

$$P(x_i, y_j, z_{k_{\text{int}}}) = p_{i,j,k_{\text{int}}}, \quad P(x_{i+1}, y_j, z_{k_{\text{int}}}) = p_{i+1,j,k_{\text{int}}}, \quad P(x_i, y_{j+1}, z_{k_{\text{int}}}) = p_{i,j+1,k_{\text{int}}},$$

$$P(x_i, y_j, z_{k_{\text{int}+1}}) = p_{i,j,k_{\text{int}}+1}, \quad P(x_{i+1}, y_{j+1}, z_{k_{\text{int}}}) = p_{i+1,j+1,k_{\text{int}}}, \quad P(x_i, y_{j+1}, z_{k_{\text{int}}+1}) = p_{i,j+1,k_{\text{int}}+1},$$

$$P(x_{i+1}, y_j, z_{k_{\text{int}}+1}) = p_{i+1,j,k_{\text{int}}+1}, \quad P(x_{i+1}, y_{j+1}, z_{k_{\text{int}}+1}) = p_{i+1,j+1,k_{\text{int}}+1};$$

- 2) continuity of the polynomial across the interface: [P] = 0 for any  $\mathbf{x} \in \mathbf{V}_{i,j,k_{\text{int}}}^{P(\mathbf{x})} \cap \{z = \xi\};$ 3) continuity of the normal fluid flux  $\varkappa \partial p/\partial x$  calculated on the polynomial  $P(\mathbf{x})$  across the interface:  $[\varkappa \partial P/\partial z] = 0$  for any  $\mathbf{x} \in \mathbf{V}_{i,j,k_{\text{int}}}^{P(\mathbf{x})} \cap \{z = \xi\}.$

Solving the system defined by conditions 1)-3) above with respect to the unknown coefficients, we obtain the following expressions:

$$a_{1}^{p} = \frac{\varkappa_{2}}{(1-\theta)\varkappa_{1} + \theta\varkappa_{2}} p_{xyz,i,j,k_{\text{int}}}, \quad b_{1}^{p} = p_{xy,i,j,k_{\text{int}}}, \quad c_{1}^{p} = \frac{\varkappa_{2}}{(1-\theta)\varkappa_{1} + \theta\varkappa_{2}} p_{xz,i,j,k_{\text{int}}},$$

$$d_{1}^{p} = \frac{\varkappa_{2}}{(1-\theta)\varkappa_{1} + \theta\varkappa_{2}} p_{yz,i,j,k_{\text{int}}}, \quad e_{1}^{p} = p_{x,i,j,k_{\text{int}}}, \quad f_{1}^{p} = p_{y,i,j,k_{\text{int}}}, \quad g_{1}^{p} = \frac{\varkappa_{2}}{(1-\theta)\varkappa_{1} + \theta\varkappa_{2}} p_{z,i,j,k_{\text{int}}};$$

$$a_{2}^{p} = \frac{\varkappa_{1}}{(1-\theta)\varkappa_{1} + \theta\varkappa_{2}} p_{xyz,i,j,k_{\text{int}}}, \quad b_{2}^{p} = p_{xy,i,j,k_{\text{int}}+1}, \quad c_{2}^{p} = \frac{\varkappa_{1}}{(1-\theta)\varkappa_{1} + \theta\varkappa_{2}} p_{xz,i,j+1,k_{\text{int}}},$$

$$d_{2}^{p} = \frac{\varkappa_{1}}{(1-\theta)\varkappa_{1} + \theta\varkappa_{2}} p_{yz,i+1,j,k_{\text{int}}}, \quad e_{2}^{p} = p_{x,i,j+1,k_{\text{int}}+1}, \quad f_{2}^{p} = p_{y,i+1,j,k_{\text{int}}+1},$$

$$g_{2}^{p} = \frac{\varkappa_{1}}{(1-\theta)\varkappa_{1} + \theta\varkappa_{2}} p_{z,i+1,j+1,k_{\text{int}}},$$

where  $p_x$ ,  $p_{xy}$ , etc. are the notations introduced in subsection 3.1.

Next, we substitute these coefficients into expression (3.11) and calculate the approximate components of the fluid velocity vector according to formulae (3.10).

If the volume  $\mathbf{V}_{i,j,k}^{P(\mathbf{x})}$  is not intersected by the interface, the interpolating polynomial P(x,y,z) is built just as an interpolation of the values in the nodes of the volume.

The resulting expressions for the fluid velocity components can be written in the following way:

$$V_{i+0.5,j,k}^{1} = -\langle \varkappa \rangle_{i+0.5,j,k}^{1} p_{\bar{x},i+1,j,k}, \quad V_{i,j+0.5,k}^{2} = -\langle \varkappa \rangle_{i,j+0.5,k}^{2} p_{\bar{y},i,j+1,k},$$

$$V_{i,j,k+0.5}^{3} = -\langle \varkappa \rangle_{i,j,k+0.5}^{3} p_{\bar{z},i,j,k+1}, \qquad (3.12)$$
where  $\langle \varkappa \rangle_{i+0.5,j,k}^{1} = \begin{cases} \varkappa_{1}, & k \leqslant k_{\text{int}}, \\ \varkappa_{2}, & k > k_{\text{int}}, \end{cases}$ 

$$\langle \varkappa \rangle_{i,j,k+0.5}^{3} = \begin{cases} \varkappa_{1}, & k \leqslant k_{\text{int}}, \\ \varkappa_{2}, & k > k_{\text{int}}, \end{cases}$$

$$\langle \varkappa \rangle_{i,j,k+0.5}^{3} = \begin{cases} \varkappa_{1}, & k \leqslant k_{\text{int}}, \\ \varkappa_{1}, & k \leqslant k_{\text{int}}, \end{cases}$$

$$\langle \varkappa \rangle_{i,j,k+0.5}^{3} = \begin{cases} \varkappa_{1}, & k \leqslant k_{\text{int}}, \\ \varkappa_{1}, & k \leqslant k_{\text{int}}, \\ \varkappa_{2}, & k > k_{\text{int}}, \end{cases}$$

$$\langle \varkappa \rangle_{i,j,k+0.5}^{3} = \begin{cases} \varkappa_{1}, & k \leqslant k_{\text{int}}, \\ \varkappa_{2}, & k > k_{\text{int}}, \\ \varkappa_{2}, & k > k_{\text{int}}, \end{cases}$$

Note that this approximation of the fluid flux in each direction is identical to the approximation of the flux in [17], where one-dimensional diffusion equation with discontinuous coefficients is considered. In fact, our discretization can be derived as a tensor product of one-dimensional ones, but the approach we present here is more general.

Next, we derive approximations of the stress tensor components needed for equations (3.7). For this purpose, we construct interpolating polynomials  $U(\mathbf{x})$ ,  $V(\mathbf{x})$ ,  $W(\mathbf{x})$  for each component of the displacement vector respectively. Then, the approximations of the stress tensor components are calculated at the appropriate grid points as follows:

$$S_{i,j,k}^{11} = \left((\lambda + 2\mu)\frac{\partial U}{\partial x} + \lambda\left(\frac{\partial V}{\partial y} + \frac{\partial W}{\partial z}\right)\right)(x_i, y_j, z_k), \quad S_{i,j,k}^{22} = \left((\lambda + 2\mu)\frac{\partial V}{\partial y} + \lambda\left(\frac{\partial U}{\partial x} + \frac{\partial W}{\partial z}\right)\right)(x_i, y_j, z_k),$$

$$S_{i,j,k}^{33} = \left((\lambda + 2\mu)\frac{\partial W}{\partial z} + \lambda\left(\frac{\partial U}{\partial x} + \frac{\partial V}{\partial y}\right)\right)(x_i, y_j, z_k), \quad S_{i+0.5,j+0.5,k}^{12} = \mu\left(\frac{\partial U}{\partial y} + \frac{\partial V}{\partial x}\right)(x_{i+0.5}, y_{j+0.5}, z_k),$$

$$S_{i+0.5,j,k+0.5}^{13} = \mu\left(\frac{\partial U}{\partial z} + \frac{\partial W}{\partial x}\right)(x_{i+0.5}, y_j, z_{k+0.5}), \quad S_{i,j+0.5,k+0.5}^{23} = \mu\left(\frac{\partial V}{\partial z} + \frac{\partial W}{\partial y}\right)(x_i, y_{j+0.5}, z_{k+0.5}).$$

$$(3.13)$$

Let us consider now the following cubic volumes built on the nodes of the grids  $G^u$ ,  $G^v$ ,  $G^w$  respectively

$$\mathbf{V}_{ijk}^{U(\mathbf{x})} = \mathbf{V}^{U(\mathbf{x})} = (x_{i-0.5}, x_{i+0.5}) \times (y_j, y_{j+1}) \times (z_k, z_{k+1}),$$

$$\mathbf{V}_{ijk}^{V(\mathbf{x})} = \mathbf{V}^{V(\mathbf{x})} = (x_i, x_{i+1}) \times (y_{j-0.5}, y_{j+0.5}) \times (z_k, z_{k+1}),$$

$$\mathbf{V}_{ijk}^{W(\mathbf{x})} = \mathbf{V}^{W(\mathbf{x})} = (x_i, x_{i+1}) \times (y_j, y_{j+1}) \times (z_{k-0.5}, z_{k+0.5}).$$
(3.14)

The volumes  $\mathbf{V}_{i,j,k}^{U(\mathbf{x})}$ ,  $\mathbf{V}_{i,j,k}^{V(\mathbf{x})}$  are intersected by the interface  $z=\xi$  when the index  $k=k_{\mathrm{int}}$ , while the volume  $\mathbf{V}_{ijk}^{W(\mathbf{x})}$  is intersected when  $k=k_{\mathrm{int}}$  and the parameter  $\theta<0.5$  or when  $k=k_{\mathrm{int}}+1$  and  $\theta>0.5$ .

Next, we subdivide each of the volumes  $\mathbf{V}_{i,j,k}^{U(\mathbf{x})}$ ,  $\mathbf{V}_{i,j,k}^{V(\mathbf{x})}$ ,  $\mathbf{V}_{i,j,k}^{W(\mathbf{x})}$  into four subdomains: two pentahedrons and two tetrahedrons (see Fig. 3.1 for the subdivision of the volume  $\mathbf{V}^{U(\mathbf{x})}$ ).

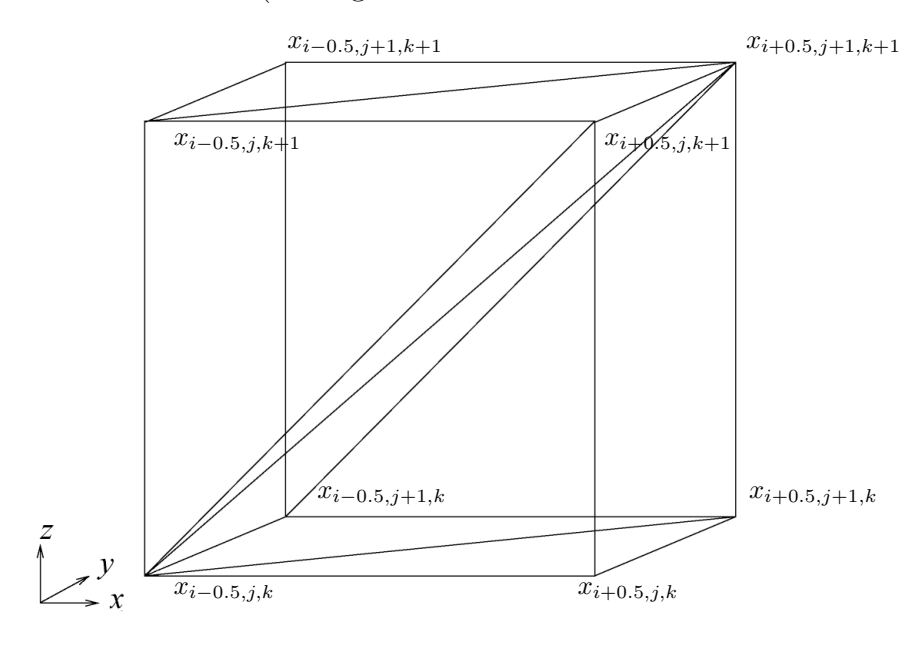


Fig. 3.1. Subdivision of the volume  $\mathbf{V}^{U(\mathbf{x})}$ 

Then, we build interpolating polynomials U(x,y,z), V(x,y,z) and W(x,y,z) in the respective subvolumes. As is seen from formulae (3.13), the approximations of the stress tensor components  $S^{11}$ ,  $S^{22}$ ,  $S^{33}$  should be calculated at the points  $\{\mathbf{x}_{i,j,k}\cap\Omega\}$ , the component  $S^{12}$  at the points  $\{\mathbf{x}_{i+0.5,j+0.5,k}\cap\Omega\}$ , the component  $S^{13}$  at the points  $\{\mathbf{x}_{i+0.5,j,k+0.5}\cap\Omega\}$ , and the component  $S^{23}$  at the points  $\{\mathbf{x}_{i,j+0.5,k+0.5}\cap\Omega\}$ . Hence, it is sufficient to build the polynomials U(x,y,z), V(x,y,z), and W(x,y,z) in the sets of pentahedrons from the subdivisions.

We choose these polynomials to be piecewise-linear, extended with one special piecewise-bilinear term in all pentahedrons, intersected by the interface, and linear ones, extended with one bilinear term otherwise. Note that these are the highest order polynomials belonging to the kernel of the linear elasticity operator. There are two types of pentahedrons for each displacement component  $\mathbf{V}_{i,j,k}^{U(\mathbf{x}),1}, \mathbf{V}_{i,j,k}^{U(\mathbf{x}),2} \subset \mathbf{V}_{i,j,k}^{U(\mathbf{x}),1}, \mathbf{V}_{i,j,k}^{V(\mathbf{x}),2}, \mathbf{V}_{i,j,k}^{V(\mathbf{x}),2} \subset \mathbf{V}_{i,j,k}^{V(\mathbf{x}),2}$ . These pentahedrons have the following vertices:

$$\mathbf{V}_{i,j,k}^{U(\mathbf{x}),1}: \{\mathbf{x}_{i-0.5,j,k}, \ \mathbf{x}_{i+0.5,j,k}, \ \mathbf{x}_{i+0.5,j+1,k}, \ \mathbf{x}_{i+0.5,j,k+1}, \ \mathbf{x}_{i+0.5,j+1,k+1} \},$$

$$\mathbf{V}_{i,j,k}^{U(\mathbf{x}),2}: \{\mathbf{x}_{i-0.5,j,k}, \ \mathbf{x}_{i-0.5,j+1,k}, \ \mathbf{x}_{i-0.5,j,k+1}, \ \mathbf{x}_{i-0.5,j+1,k+1}, \ \mathbf{x}_{i+0.5,j+1,k+1}\}, \\ \mathbf{V}_{i,j,k}^{V(\mathbf{x}),1}: \{\mathbf{x}_{i,j-0.5,k}, \ \mathbf{x}_{i,j+0.5,k}, \ \mathbf{x}_{i,j+0.5,k+1}, \ \mathbf{x}_{i+1,j+0.5,k}, \ \mathbf{x}_{i+1,j+0.5,k+1}\}, \\ \mathbf{V}_{i,j,k}^{V(\mathbf{x}),2}: \{\mathbf{x}_{i,j-0.5,k}, \ \mathbf{x}_{i,j-0.5,k+1}, \ \mathbf{x}_{i+1,j-0.5,k}, \ \mathbf{x}_{i+1,j-0.5,k+1}, \ \mathbf{x}_{i+1,j+0.5,k+1}\}, \\ \mathbf{V}_{i,j,k}^{W(\mathbf{x}),1}: \{\mathbf{x}_{i,j,k-0.5}, \ \mathbf{x}_{i,j,k+0.5}, \ \mathbf{x}_{i+1,j,k+0.5}, \ \mathbf{x}_{i,j+1,k+0.5}, \ \mathbf{x}_{i+1,j+1,k+0.5}\}, \\ \mathbf{V}_{i,j,k}^{W(\mathbf{x}),2}: \{\mathbf{x}_{i,j,k-0.5}, \ \mathbf{x}_{i+1,j,k-0.5}, \ \mathbf{x}_{i,j+1,k-0.5}, \ \mathbf{x}_{i+1,j+1,k-0.5}, \ \mathbf{x}_{i+1,j+1,k+0.5}\}.$$

In the pentahedrons intersected by the interface (it happens if and only if the corresponding cubic volume is intersected), the polynomials should fulfill the continuity conditions on the interface.

Let us consider three such neighboring pentahedrons  $\mathbf{V}_{i,j,k_{\mathrm{int}}}^{U(\mathbf{x}),1}, \mathbf{V}_{i,j,k_{\mathrm{int}}}^{V(\mathbf{x}),1}$ , and  $\mathbf{V}_{i,j,k_{\mathrm{int}}}^{W(\mathbf{x}),1}$  in the case where the parameter  $\theta$  satisfies  $\theta < 0.5$ . In this case, the interface  $\xi$  is located between the coordinates  $z_{k_{\rm int}}$  and  $z_{k_{\rm int}+0.5}$ , and hence these three pentahedrons are intersected by the interface. The general representation of the polynomials in these tetrahedrons can be written as follows:

$$U(x,y,z) = \begin{cases} a_1^u(y-y_j)(z-z_{k_{\text{int}}}) + b_1^u(x-x_{i-0.5}) + c_1^u(y-y_j) + \\ d_1^u(z-z_{k_{\text{int}}}) + u_{i-0.5,j,k_{\text{int}}}, & \mathbf{x} \in \mathbf{V}_{i,j,k_{\text{int}}}^{U(\mathbf{x}),1} \cap (z < \xi), \\ a_2^u(y-y_j)(z-z_{k_{\text{int}}+1}) + b_2^u(x-x_{i+0.5}) + c_2^u(y-y_j) + \\ d_2^u(z-z_{k_{\text{int}}+1}) + u_{i+0.5,j,k_{\text{int}}+1}, & \mathbf{x} \in \mathbf{V}_{i,j,k_{\text{int}}}^{U(\mathbf{x}),1} \cap (z > \xi), \end{cases}$$
(3.15)

$$V(x,y,z) = \begin{cases} a_1^v(x-x_i)(z-z_{k_{\text{int}}}) + b_1^v(x-x_i) + c_1^v(y-y_{j-0.5}) + \\ d_1^v(z-z_{k_{\text{int}}}) + v_{i,j-0.5,k_{\text{int}}}, & \mathbf{x} \in \mathbf{V}_{i,j,k_{\text{int}}}^{V(\mathbf{x}),1} \cap (z < \xi), \\ a_2^v(x-x_i)(z-z_{k_{\text{int}}+1}) + b_2^v(x-x_i) + c_2^v(y-y_{j+0.5}) + \\ d_2^v(z-z_{k_{\text{int}}+1}) + v_{i,j+0.5,k_{\text{int}}+1}, & \mathbf{x} \in \mathbf{V}_{i,j,k_{\text{int}}}^{V(\mathbf{x}),1} \cap (z > \xi), \end{cases}$$
(3.16)

$$V(x,y,z) = \begin{cases} a_1^v(x-x_i)(z-z_{k_{\text{int}}}) + b_1^v(x-x_i) + c_1^v(y-y_{j-0.5}) + \\ d_1^v(z-z_{k_{\text{int}}}) + v_{i,j-0.5,k_{\text{int}}}, & \mathbf{x} \in \mathbf{V}_{i,j,k_{\text{int}}}^{V(\mathbf{x}),1} \cap (z < \xi), \\ a_2^v(x-x_i)(z-z_{k_{\text{int}}+1}) + b_2^v(x-x_i) + c_2^v(y-y_{j+0.5}) + \\ d_2^v(z-z_{k_{\text{int}}+1}) + v_{i,j+0.5,k_{\text{int}}+1}, & \mathbf{x} \in \mathbf{V}_{i,j,k_{\text{int}}}^{V(\mathbf{x}),1} \cap (z > \xi), \end{cases}$$

$$W(x,y,z) = \begin{cases} a_1^w(x-x_i)(y-y_j) + b_1^w(x-x_i) + c_1^w(y-y_j) + \\ d_1^w(z-z_{k_{\text{int}}-0.5}) + w_{i,j,k_{\text{int}}-0.5}, & \mathbf{x} \in \mathbf{V}_{i,j,k_{\text{int}}}^{V(\mathbf{x}),1} \cap (z < \xi), \\ a_2^w(x-x_i)(y-y_j) + b_2^w(x-x_i) + c_2^w(y-y_j) + \\ qd_2^w(z-z_{k_{\text{int}}+0.5}) + w_{i,j,k_{\text{int}}+0.5}, & \mathbf{x} \in \mathbf{V}_{i,j,k_{\text{int}}}^{V(\mathbf{x}),1} \cap (z > \xi). \end{cases}$$

$$(3.16)$$

The unknown coefficients of polynomials (3.15)-(3.17) can be determined from the following conditions:

1) interpolation at the vertices of the pentahedrons

$$\begin{split} U(x_{i-0.5},y_j,z_{k_{\mathrm{int}}}) &= u_{i-0.5,j,k_{\mathrm{int}}}, \quad U(x_{i+0.5},y_j,z_{k_{\mathrm{int}}}) = u_{i+0.5,j,k_{\mathrm{int}}}, \\ U(x_{i+0.5},y_{j+1},z_{k_{\mathrm{int}}}) &= u_{i+0.5,j+1,k_{\mathrm{int}}}, \quad U(x_{i+0.5},y_j,z_{k_{\mathrm{int}}+1}) = u_{i+0.5,j,k_{\mathrm{int}}+1}, \\ U(x_{i+0.5},y_{j+1},z_{k_{\mathrm{int}}+1}) &= u_{i+0.5,j+1,k_{\mathrm{int}}+1}, \\ V(x_i,y_{j-0.5},z_{k_{\mathrm{int}}}) &= v_{i,j-0.5,k_{\mathrm{int}}}, \quad V(x_i,y_{j+0.5},z_{k_{\mathrm{int}}}) = v_{i,j+0.5,k_{\mathrm{int}}}, \\ V(x_{i+1},y_{j+0.5},z_{k_{\mathrm{int}}}) &= v_{i+1,j+0.5,k_{\mathrm{int}}+1}, \\ V(x_{i+1},y_{j+0.5},z_{k_{\mathrm{int}}+1}) &= v_{i+1,j+0.5,k_{\mathrm{int}}+1}, \end{split}$$

$$W(x_i, y_j, z_{k_{\text{int}}-0.5}) = w_{i,j,k_{\text{int}}-0.5}, \quad W(x_i, y_j, z_{k_{\text{int}}+0.5}) = w_{i,j,k_{\text{int}}+0.5},$$

$$W(x_{i+1}, y_j, z_{k_{\text{int}}+0.5}) = w_{i+1,j,k_{\text{int}}+0.5}, \quad W(x_i, y_{j+1}, z_{k_{\text{int}}+0.5}) = w_{i,j+1,k_{\text{int}}+0.5},$$

$$W(x_{i+1}, y_{j+1}, z_{k_{\text{int}}+0.5}) = w_{i+1,j+1,k_{\text{int}}+0.5};$$

2) continuity of all displacement components across the interface

$$[U] = 0, \text{ for any } \mathbf{x} \in \mathbf{V}_{i,j,k_{\text{int}}}^{U(\mathbf{x}),1} \cap \{z = \xi\},$$
$$[V] = 0, \text{ for any } \mathbf{x} \in \mathbf{V}_{i,j,k_{\text{int}}}^{V(\mathbf{x}),1} \cap \{z = \xi\},$$
$$[W] = 0, \text{ for any } \mathbf{x} \in \mathbf{V}_{i,j,k_{\text{int}}}^{W(\mathbf{x}),1} \cap \{z = \xi\};$$

3) continuity of the normal components of the stress tensor across the interface

$$\left[\mu\left(\frac{\partial U}{\partial z} + \frac{\partial W}{\partial x}\right)\right] = 0, \text{ for any } \mathbf{x} \in \mathbf{V}_{i,j,k_{\mathrm{int}}}^{U(\mathbf{x}),1} \cap \mathbf{V}_{i,j,k_{\mathrm{int}}}^{W(\mathbf{x}),1} \cap \{z = \xi\},$$

$$\left[\mu\left(\frac{\partial V}{\partial z} + \frac{\partial W}{\partial y}\right)\right] = 0, \text{ for any } \mathbf{x} \in \mathbf{V}_{i,j,k_{\mathrm{int}}}^{V(\mathbf{x}),1} \cap \mathbf{V}_{i,j,k_{\mathrm{int}}}^{W(\mathbf{x}),1} \cap \{z = \xi\},$$

$$\left[(\lambda + 2\mu)\frac{\partial W}{\partial z} + \lambda\left(\frac{\partial U}{\partial x} + \frac{\partial V}{\partial y}\right)\right] = 0, \text{ for any } \mathbf{x} \in \mathbf{V}_{i,j,k_{\mathrm{int}}}^{U(\mathbf{x}),1} \cap \mathbf{V}_{i,j,k_{\mathrm{int}}}^{V(\mathbf{x}),1} \cap \mathbf{V}_{i,j,k_{\mathrm{int}}}^{W(\mathbf{x}),1} \cap \{z = \xi\}.$$

Conditions 1)-3) result in the following expressions for the coefficients of the polynomials (3.15)-(3.17):

$$a_{1}^{u} = \frac{(\theta - 1)(\mu_{1} - \mu_{2})w_{xy,i,j,k_{\text{int}}+0.5} + \mu_{2}u_{yz,i+0.5,j,k_{\text{int}}}}{(1 - \theta)\mu_{1} + \theta\mu_{2}}, \quad b_{1}^{u} = u_{x,i-0.5,j,k_{\text{int}}},$$

$$d_{1}^{u} = \frac{\mu_{2}u_{z,i+0.5,j,k_{\text{int}}} + (\theta - 1)(\mu_{1} - \mu_{2})w_{x,i,j,k_{\text{int}}+0.5}}{(1 - \theta)\mu_{1} + \theta\mu_{2}}, \quad c_{1}^{u} = u_{y,i+0.5,j,k_{\text{int}}},$$

$$a_{2}^{u} = \frac{\theta(\mu_{1} - \mu_{2})w_{xy,i,j,k_{\text{int}}+0.5} + \mu_{1}u_{yz,i+0.5,j,k_{\text{int}}}}{(1 - \theta)\mu_{1} + \theta\mu_{2}}, \quad b_{2}^{u} = u_{x,i-0.5,j,k_{\text{int}}},$$

$$d_{2}^{u} = \frac{\mu_{1}u_{z,i+0.5,j,k_{\text{int}}} + \theta(\mu_{1} - \mu_{2})w_{x,i,j,k_{\text{int}}+0.5}}{(1 - \theta)\mu_{1} + \theta\mu_{2}}, \quad c_{2}^{u} = u_{y,i+0.5,j,k_{\text{int}}+1},$$

$$a_{1}^{v} = \frac{(\theta - 1)(\mu_{1} - \mu_{2})w_{xy,ij,k_{\text{int}}+0.5} + \mu_{2}v_{xz,i,j+0.5,k_{\text{int}}}}{(1 - \theta)\mu_{1} + \theta\mu_{2}}, \quad b_{1}^{v} = v_{x,i,j+0.5,k_{\text{int}}},$$

$$d_{1}^{v} = \frac{\mu_{2}v_{z,ij+0.5k_{\text{int}}} + (\theta - 1)(\mu_{1} - \mu_{2})w_{y,i,j,k_{\text{int}}+0.5}}{(1 - \theta)\mu_{1} + \theta\mu_{2}}, \quad c_{1}^{v} = v_{y,i,j-0.5,k_{\text{int}}},$$

$$d_{2}^{v} = \frac{\theta(\mu_{1} - \mu_{2})w_{xy,ij,k_{\text{int}}+0.5} + \mu_{2}v_{xz,ij+0.5k_{\text{int}}}}{(1 - \theta)\mu_{1} + \theta\mu_{2}}, \quad c_{2}^{v} = v_{x,i,j+0.5,k_{\text{int}}+1},$$

$$d_{2}^{v} = \frac{\theta(\mu_{1} - \mu_{2})w_{xy,ij,k_{\text{int}}+0.5} + \mu_{2}v_{xz,ij+0.5k_{\text{int}}}}{(1 - \theta)\mu_{1} + \theta\mu_{2}}, \quad c_{2}^{v} = v_{y,i,j-0.5,k_{\text{int}}+1},$$

$$d_{2}^{v} = \frac{\theta(\mu_{1} - \mu_{2})w_{xy,ij,k_{\text{int}}+0.5} + \mu_{2}v_{xz,ij+0.5k_{\text{int}}}}{(1 - \theta)\mu_{1} + \theta\mu_{2}}, \quad c_{2}^{v} = v_{y,i,j-0.5,k_{\text{int}}+1},$$

$$d_{2}^{v} = \frac{\theta(\mu_{1} - \mu_{2})w_{xy,ij,k_{\text{int}}+0.5} + \mu_{2}v_{xz,ij+0.5k_{\text{int}}}}{(1 - \theta)\mu_{1} + \theta\mu_{2}}, \quad c_{2}^{v} = v_{y,i,j-0.5,k_{\text{int}}+1},$$

$$d_{1}^{v} = \frac{\theta(\mu_{1} - \mu_{2})w_{xy,ij,k_{\text{int}}+0.5}}{(1 - \theta)\mu_{1} + \theta\mu_{2}}, \quad c_{2}^{v} = v_{y,i,j-0.5,k_{\text{int}}+1},$$

$$d_{1}^{v} = \frac{\theta(\mu_{1} - \mu_{2})w_{xy,ij,k_{\text{int}}+0.5}}{(1 - \theta)\mu_{1} + \theta\mu_{2}}, \quad c_{2}^{v} = v_{y,i,j-0.5,k_{\text{int}}+1},$$

$$d_{1}^{v} = \frac{\theta(\mu_{1} - \mu_{2})w_{xy,ij,k_{\text{int}}+0.5}}{(1 - \theta)\mu_{1} + \theta\mu_{2}}, \quad c_{2}^{v} = v_{y,i,j-0.5,k_{\text{int}}+1},$$

$$d_{1}^{v} = \frac{\theta(\mu_{1} - \mu_{2})w_{xy,ij,k_{\text{int}}+0.5}}{(1 - \theta)\mu_{1} + \theta\mu_{2}}, \quad c_{2}^{v} = v_{y,$$

$$a_2^w = w_{xy,i,j,k_{\text{int}}+0.5}, \quad b_2^w = w_{x,i,j,k_{\text{int}}+0.5}, \quad c_2^w = w_{y,i,j,k_{\text{int}}+0.5},$$

$$d_2^w = \frac{(\lambda_1 + 2\mu_1)w_{z,i,j,k_{\text{int}}-0.5} + (\theta + 0.5)(\lambda_1 - \lambda_2)(u_{x,i-0.5,j,k_{\text{int}}} + v_{y,i,j-0.5,k_{\text{int}}})}{(0.5 - \theta)(\lambda_1 + 2\mu_1) + (0.5 + \theta)(\lambda_2 + 2\mu_2)}.$$

Then, upon substitution of these coefficients into the expressions for the polynomials (3.15) – (3.17), we calculate the approximate stress tensor components using formulae (3.13).

In a similar way, we consider the case that  $\theta \ge 0.5$ . In the case where the pentahedrons are not intersected by the interface, the polynomials are derived only as interpolation of the values at the vertices. In the volumes adjacent to the boundary  $\Gamma$ , the proper boundary conditions are taken into account as well.

Summarizing all the cases mentioned above, the approximations for the stress tensor components can be written in the following way:

$$S_{i+0.5,j+0.5,k}^{12} = \langle \mu \rangle_{i+0.5,j+0.5,k}^{uv} (u_{y,i+0.5,j,k} + v_{x,i,j+0.5,k}),$$

$$S_{i+0.5,j,k+0.5}^{13} = \langle \mu \rangle_{i+0.5,j,k+0.5}^{uw} (u_{z,i+0.5,j,k} + w_{x,i,j,k+0.5}),$$

$$S_{i,j+0.5,k+0.5}^{23} = \langle \mu \rangle_{i,j+0.5,k+0.5}^{vw} (v_{z,i,j+0.5,k} + w_{y,i,j,k+0.5}),$$

$$S_{i,j,k}^{11} = (\langle \lambda \rangle_{i,j,k}^{u} + 2\mu_{1}) u_{x,i-0.5,j,k} + \langle \lambda \rangle_{ijk}^{v} v_{y,i,j-0.5,k} + \langle \lambda \rangle_{i,j,k}^{w} w_{z,i,j,k-0.5},$$

$$S_{i,j,k}^{22} = (\langle \lambda \rangle_{i,j,k}^{v} + 2\mu_{1}) v_{y,i,j-0.5,k} + \langle \lambda \rangle_{i,j,k}^{u} u_{x,i-0.5,j,k} + \langle \lambda \rangle_{i,j,k}^{w} w_{z,i,j,k-0.5},$$

$$S_{i,j,k}^{33} = \langle \lambda + 2\mu \rangle_{ijk}^{w} w_{z,i,j,k-0.5} + \langle \lambda \rangle_{i,j,k}^{uv} (u_{x,i-0.5,j,k} + v_{y,i,j-0.5,k}),$$
(3.18)

where

$$\langle \mu \rangle_{i+0.5,j+0.5,k}^{uv} = \begin{cases} \mu_1, & k \leqslant k_{\text{int}}, \\ \mu_2, & k > k_{\text{int}}, \end{cases}$$

$$\langle \mu \rangle_{i+0.5,j,k+0.5}^{uw} = \langle \mu \rangle_{i,j+0.5,k+0.5}^{vw} = \begin{cases} \mu_1, & k < k_{\text{int}}, \\ \frac{\mu_1 \mu_2}{(1-\theta)\mu_1 + \theta \mu_2}, & k = k_{\text{int}}, \\ \mu_2, & k > k_{\text{int}} + 1, \end{cases}$$

$$\langle \lambda \rangle_{i,j,k}^{u} = \langle \lambda \rangle_{i,j,k}^{v} = \begin{cases} \lambda_{1}, & k < k_{\text{int}} \text{ or } k = k_{\text{int}}, \ \theta > 0.5, \\ \lambda_{1} \frac{(0.5 - \theta)(\lambda_{2} + 2\mu_{1}) + (0.5 + \theta)(\lambda_{2} + 2\mu_{2})}{(0.5 - \theta)(\lambda_{1} + 2\mu_{1}) + (0.5 + \theta)(\lambda_{2} + 2\mu_{2})}, & k = k_{\text{int}}, \ \theta < 0.5, \\ \lambda_{2} \frac{(\theta - 0.5)(\lambda_{1} + 2\mu_{2}) + (1.5 - \theta)(\lambda_{1} + 2\mu_{1})}{(1.5 - \theta)(\lambda_{1} + 2\mu_{1}) + (\theta - 0.5)(\lambda_{2} + 2\mu_{2})}, & k = k_{\text{int}} + 1, \ \theta > 0.5, \\ \lambda_{2}, & k > k_{\text{int}} + 1, \text{ or } k = k_{\text{int}} + 1, \ \theta < 0.5, \end{cases}$$

$$\langle \lambda \rangle_{i,j,k}^{w} = \begin{cases} \lambda_{1}, & k < k_{\text{int}}, \text{ or } k = k_{\text{int}}, \ \theta > 0.5, \\ \lambda_{1} \frac{\lambda_{2} + 2\mu_{2}}{(0.5 - \theta)(\lambda_{1} + 2\mu_{1}) + (0.5 + \theta)(\lambda_{2} + 2\mu_{2})}, & k = k_{\text{int}}, \ \theta < 0.5, \\ \lambda_{2} \frac{\lambda_{1} + 2\mu_{1}}{(1.5 - \theta)(\lambda_{1} + 2\mu_{1}) + (\theta - 0.5)(\lambda_{2} + 2\mu_{2})}, & k = k_{\text{int}} + 1, \ \theta > 0.5, \\ \lambda_{2}, & k > k_{\text{int}} + 1, \text{ or } k = k_{\text{int}} + 1, \ \theta < 0.5, \end{cases}$$

$$\langle \lambda \rangle_{i,j,k}^{uv} = \begin{cases} \lambda_1, & k < k_{\text{int}}, \text{ or } k = k_{\text{int}}, \ \theta > 0.5, \\ \frac{(0.5 - \theta)(\lambda_1 + 2\mu_1)\lambda_2 + (0.5 + \theta)(\lambda_2 + 2\mu_2)\lambda_1}{(0.5 - \theta)(\lambda_1 + 2\mu_1) + (0.5 + \theta)(\lambda_2 + 2\mu_2)}, & k = k_{\text{int}}, \ \theta < 0.5, \\ \frac{(1.5 - \theta)(\lambda_1 + 2\mu_1)\lambda_2 + (\theta - 0.5)(\lambda_2 + 2\mu_2)\lambda_1}{(1.5 - \theta)(\lambda_1 + 2\mu_1) + (\theta - 0.5)(\lambda_2 + 2\mu_2)}, & k = k_{\text{int}} + 1, \ \theta > 0.5, \\ \lambda_2, & k > k_{\text{int}} + 1, \text{ or } k = k_{\text{int}} + 1, \ \theta < 0.5, \end{cases}$$

$$\langle \lambda + 2\mu \rangle_{i,j,k}^{w} = \begin{cases} \lambda_{1} + 2\mu_{1}, & k < k_{\text{int}}, \text{ or } k = k_{\text{int}}, \ \theta > 0.5, \\ \frac{(\lambda_{1} + 2\mu_{1})(\lambda_{2} + 2\mu_{2})}{(0.5 - \theta)(\lambda_{1} + 2\mu_{1}) + (0.5 + \theta)(\lambda_{2} + 2\mu_{2})}, & k = k_{\text{int}}, \ \theta < 0.5, \\ \frac{(\lambda_{1} + 2\mu_{1})(\lambda_{2} + 2\mu_{2})}{(1.5 - \theta)(\lambda_{1} + 2\mu_{1}) + (\theta - 0.5)(\lambda_{2} + 2\mu_{2})}, & k = k_{\text{int}} + 1, \ \theta > 0.5, \\ \lambda_{2} + 2\mu_{2}, & k > k_{\text{int}} + 1, \text{ or } k = k_{\text{int}} + 1, \ \theta < 0.5, \end{cases}$$

$$\langle \lambda + 2\mu \rangle_{i,j,k}^u = \langle \lambda \rangle_{i,j,k}^u + 2\mu_{i,j,k}, \quad \langle \lambda + 2\mu \rangle_{i,j,k}^v = \langle \lambda \rangle_{i,j,k}^v + 2\mu_{i,j,k}.$$

Now, we substitute the derived approximating expressions for the stress tensor components (3.18) and the fluid velocity components (3.12) into equations (3.7) and obtain a discrete system of equations for the unknown grid functions u, v, w, p

$$-(\langle \lambda + 2\mu \rangle_{i,j,k}^{u} u_{\bar{x},i+0.5,j,k} + \langle \lambda \rangle_{i,j,k}^{v} v_{\bar{y},i,j+0.5,k} + \langle \lambda \rangle_{i,j,k}^{w} w_{\bar{z},i,j,k+0.5} \rangle_{x} - (\mu_{i+0.5,j-0.5,k} \times (u_{\bar{y},i+0.5,j,k} + v_{\bar{x},i+1,j-0.5,k}))_{y} - (\langle \mu \rangle_{i+0.5,j,k-0.5}^{uw} (u_{\bar{z},i+0.5,j,k} + w_{\bar{x},i+1,j,k-0.5}))_{z} + p_{\bar{x},i,j,k} = 0,$$

$$-(\langle \lambda + 2\mu \rangle_{i,j,k}^{v} v_{\bar{y},i,j+0.5,k} + \langle \lambda \rangle_{i,j,k}^{u} u_{\bar{x},i+0.5,j,k} + \langle \lambda \rangle_{i,j,k}^{w} w_{\bar{z},i,j,k+0.5})_{y} - (\mu_{i-0.5,j+0.5,k} \times (v_{\bar{x},i+1,j+0.5,k} + u_{\bar{y},i-0.5,j+1,k}))_{x} - (\langle \mu \rangle_{i,j+0.5,k-0.5}^{vw} (v_{\bar{z},i,j+0.5,k} + w_{\bar{y},i,j+1,k-0.5}))_{z} + p_{\bar{y},i,j,k} = 0,$$

$$-(\langle \lambda + 2\mu \rangle_{i,j,k}^{w} w_{\bar{z},i,j,k+0.5} + \langle \lambda \rangle_{i,j,k}^{uv} (u_{\bar{x},i+0.5,j,k} + v_{\bar{y},i,j+0.5,k}))_{z} - (\langle \mu \rangle_{i-0.5,j,k+0.5}^{uw} \times (w_{\bar{x},i,j,k+0.5} + u_{\bar{z},i-0.5,j,k+1}))_{x} - (\langle \mu \rangle_{i,j-0.5,k+0.5}^{vw} (w_{\bar{y},i,j,k+0.5} + v_{\bar{z},i,j-0.5,k+1}))_{y} + p_{\bar{z},i,j,k} = 0,$$

$$(\langle \alpha \rangle_{i,j,k} p_{i,j,k} + u_{x,i-0.5,j,k} + v_{y,i,j-0.5,k} + w_{z,i,j,k-0.5})_{t} - (\langle \varkappa \rangle_{i-0.5,j,k}^{1} p_{\bar{x}}^{\sigma})_{x} - (\langle \varkappa \rangle_{i,j-0.5,k}^{2} p_{\bar{y}}^{\sigma})_{y} - (\langle \varkappa \rangle_{i-0.5,j,k}^{3} p_{\bar{z}}^{\sigma})_{z} = \langle f \rangle_{i,j,k}^{\sigma},$$

$$(3.19)$$

where  $\langle a \rangle$  and  $\langle f \rangle$  are calculated according to formulae (3.8).

Note that finite volume methods are known for their property to preserve the fluxes of the problem and produce so-called conservative discretizations. The derived finite difference scheme (3.19) is hence conservative due to the derivation. Yet, the matrix of the obtained system can be nonsymmetric due to the specific averagings of the coefficients in the stresses  $S^{11}$ ,  $S^{22}$ , and  $S^{33}$  which can produce, e.g., different coefficients before the mixed derivative  $w_{\bar{z}x}$  (in the first equation) and before  $u_{\bar{x}z}$  (in the third equation).

To our knowledge, no such scheme has been derived before. In the case of constant coefficients, the scheme is identical with the finite difference scheme from [21], where the Biot model in a homogeneous porous medium is considered.

# 4. Numerical experiments

In this article, we present a set of numerical experiments based on the discrete model (3.19). First, we show that the derived method is exact for piecewise-continuous polynomials of certain order. Second, we study the convergence for both the basic unknowns of the problem (displacement components and pressure) and the fluxes of the problem (components of the stress tensor and the fluid velocity) with respect to an exact solution of a continuous problem. And finally, we consider certain physical phenomena that can be described by the Biot system with discontinuous coefficients (in this case, the exact solution is unknown) and calculate the physical characteristics of the process.

**Example 4.1.** This example shows that our method is exact if the solution of problems (2.11), (2.12) is represented by certain polynomials. In particular, these polynomials should be piecewise-linear, extended with one special piecewise-bilinear term for each displacement component, and piecewise-trilinear for pressure. E.g., the following polynomials are of this kind:

$$\begin{split} U^{\text{ex}}(x,y,z) &= \left\{ \begin{array}{l} yz + x + y + z + 1, & 0 < z < \xi, \\ \frac{2\mu_1 - \mu_2}{\mu_2} yz + x + \frac{2\mu_2 \xi + \mu_2 - 2\mu_1 \xi}{\mu_2} y + 2z + 1 - \xi, & \xi < z < 1, \\ V^{\text{ex}}(x,y,z) &= \left\{ \begin{array}{l} xz + x + \frac{3\lambda_2 + 4\mu_2 - 2\lambda_1 - 2\mu_1}{\lambda_1 - \lambda_2} y + z + 1, & 0 < z < \xi, \\ \frac{2\mu_1 - \mu_2}{\mu_2} xz + \frac{2\xi\mu_2 - 2\xi\mu_1 + \mu_2}{\mu_2} x + \\ \frac{3\lambda_2 + 4\mu_2 - 2\lambda_1 - 2\mu_1}{\lambda_1 - \lambda_2} y + 2z + 1 - \xi, & \xi < z < 1, \\ W^{\text{ex}}(x,y,z) &= \left\{ \begin{array}{l} xy + \frac{\mu_1 - 2\mu_2}{\mu_2 - \mu_1} x + \frac{\mu_1 - 2\mu_2}{\mu_2 - \mu_1} y + z + 1, & 0 < z < \xi, \\ xy + \frac{\mu_1 - 2\mu_2}{\mu_2 - \mu_1} x + \frac{\mu_1 - 2\mu_2}{\mu_2 - \mu_1} y + 2z + 1 - \xi, & \xi < z < 1, \\ P^{\text{ex}}(x,y,z) &= \left\{ \begin{array}{l} \varkappa_2 xy(z - \xi), & 0 < z < \xi, \\ \varkappa_1 xy(z - \xi), & \xi < z < 1. \end{array} \right. \end{split}$$

The initial conditions are prescribed from the exact solution and the values for the boundary conditions are calculated from the exact solution and are as follows:

$$p(\mathbf{x},t) = P^{\mathrm{ex}}(\mathbf{x},t), \quad \mathbf{x} \in \Gamma,$$

$$\frac{\partial u}{\partial x} = \frac{\partial U^{\mathrm{ex}}}{\partial x}, \quad v = V^{\mathrm{ex}}, \quad w = W^{\mathrm{ex}}, \quad \text{at} \quad x = 0, 1,$$

$$u = U^{\mathrm{ex}}, \quad \frac{\partial v}{\partial y} = \frac{\partial V^{\mathrm{ex}}}{\partial y}, \quad w = W^{\mathrm{ex}}, \quad \text{at} \quad y = 0, 1,$$

$$u = U^{\mathrm{ex}}, \quad v = V^{\mathrm{ex}}, \quad \frac{\partial w}{\partial z} = \frac{\partial W^{\mathrm{ex}}}{\partial z}, \quad \text{at} \quad z = 0, 1.$$

After discretization (3.19) is performed, we vary the coefficients  $\lambda_1$ ,  $\lambda_2$ ,  $\mu_1$ ,  $\mu_2$ ,  $\varkappa_1$ ,  $\varkappa_2$  and solve the obtained linear system with an iterative solver. The results of the experiments show that the solver always converges after the first iteration and produces a solution that is exact at the grid points.

 $32^{3}$ 

 $64^{3}$ 

rate

4.0

4.0

2.0

0.9205E - 04

0.2317E - 04

**Example 4.2.** In this example, we choose the exact solution of the continuous problem (2.11), (2.12) as follows:

$$u^{\text{ex}}(x,y,z,t) = \begin{cases} \mu_1^{-1}\cos(\pi x)y\sin(z-\xi)e^{-t}, & 0 < z < \xi, \\ \mu_2^{-1}\cos(\pi x)y\sin(z-\xi)e^{-t}, & \xi < z < 1, \end{cases}$$

$$v^{\text{ex}}(x,y,z,t) = \begin{cases} \mu_1^{-1}x\cos(\pi y)\sin(z-\xi)e^{-t}, & 0 < z < \xi, \\ \mu_2^{-1}x\cos(\pi y)\sin(z-\xi)e^{-t}, & 0 < z < \xi, \\ \mu_2^{-1}x\cos(\pi y)\sin(z-\xi)e^{-t}, & \xi < z < 1, \end{cases}$$

$$w^{\text{ex}}(x,y,z,t) = \begin{cases} (\lambda_1 + 2\mu_1)^{-1}xy\sin(z-\xi)e^{-t}, & 0 < z < \xi, \\ (\lambda_2 + 2\mu_2)^{-1}xy\sin(z-\xi)e^{-t}, & \xi < z < 1, \end{cases}$$

$$p^{\text{ex}}(x,y,z,t) = \begin{cases} \varkappa_1^{-1}xy(z-\xi)\sin(z)e^{-t}, & 0 < z < \xi, \\ \varkappa_2^{-1}xy(z-\xi)\sin(z)e^{-t}, & \xi < z < 1. \end{cases}$$

The exact solutions for the stress tensor and the fluid velocity vector are calculated using the solutions  $u^{\text{ex}}$ ,  $v^{\text{ex}}$ ,  $v^{\text{ex}}$ ,  $p^{\text{ex}}$  according to formulae (2.2), (2.3) respectively.

The boundary and initial conditions are calculated in the same way as described in Example 4.1. The right hand sides of the equations are calculated by substituting the exact solution into the system.

The following values of the parameters are chosen in this experiment: T = 0.001,  $\xi = 0.5001$ , and a = 0 (fluid is incompressible). We assign the time discretization parameter  $\sigma = 1$ , which corresponds to the fully-implicit discretization in time.

In our numerical experiments, we compare the numerical solutions calculated on different grids to the known analytical solutions and calculate the relative discrete  $L_2$ -norm and the relative discrete maximum norm (C-norm) of errors of the solution.

In the experiments, we prescribe  $h_x = h_y = h_z$  and use only one time step, i.e.,  $\tau = T$ . Since the time interval T is rather small, this means that the time step  $\tau$  is rather small. Usually, the poroelasticity problem with a small time step is more difficult to solve numerically and it often results in artificial oscillations of the pressure at the first time steps of the process. Note that, on the other hand, a small time step guarantees that during the thickening of the mesh in space there is no dominance of the error part depending on the time step  $\tau$ .

**Example 4.3.** In this example, coefficients  $\lambda$ ,  $\mu$  and  $\varkappa$  experience jumps of six orders of magnitude:  $\lambda_1 = 1$ ,  $\mu_1 = 1$ ,  $\varkappa_1 = 1$ ,  $\lambda_2 = 10^6$ ,  $\mu_2 = 10^6$ ,  $\varkappa_2 = 10^6$ .

The convergence results for this set of parameters are summarized in Tables 4.1-4.4. One can see from the tables that the second order of convergence is observed for primary unknowns (u, v, w and p) as well as for the fluxes of the problem (stress tensor and fluid velocity components).

grid	$\ \varepsilon_u\ _c$	ratio	$\ \varepsilon_v\ _c$	ratio	$\ \varepsilon_w\ _c$	ratio	$\ \varepsilon_p\ _c$	ratio
$8^{3}$	0.1336E - 02	_	0.1336E - 02	_	0.2259E - 02	_	0.4182E - 02	_
$16^{3}$	0.3639E - 03	3.7	0.3639E - 03	3.7	0.6016E - 03	3.8	0.1074E - 02	3.9

4.0

4.0

2.0

0.1525E - 03

0.3847E - 04

3.9

4.0

2.0

0.2805E - 03

0.6944E - 04

3.8

4.0

2.0

Table 4.1. Convergence of u, v, w, p in the maximum norm (Example 4.1)

Table 4.2. Convergence of the stress tensor components in the maximum norm (Example 4.1)

grid	$\ arepsilon_{S^{11}}\ _c$	ratio	$\ arepsilon_{S^{22}}\ _c$	ratio	$\ arepsilon_{S^{33}}\ _c$	ratio
$8^{3}$	0.1482E - 01	_	0.1482E - 01	_	0.1877E - 01	_
$16^{3}$	0.5440E - 02	2.7	0.5440E - 02	2.7	0.4870E - 02	3.9
$32^{3}$	0.1606E - 02	3.4	0.1606E - 02	3.4	0.1235E - 02	3.9
$64^{3}$	0.4306E - 03	3.7	0.4306E - 03	3.7	0.3080E - 03	4.0
rate	_	1.9	_	1.9	_	2.0

Table 4.3. Convergence of the stress tensor components in the maximum norm (Example 4.1)

grid	$\ arepsilon_{S^{12}}\ _c$	ratio	$\ arepsilon_{S^{13}}\ _c$	ratio	$\ arepsilon_{S^{23}}\ _c$	ratio
$8^{3}$	0.1367E - 01	_	0.1947E - 01	_	0.1947E - 01	
$16^{3}$	0.4573E - 02	3.0	0.5041E - 02	3.9	0.5041E - 02	3.9
$32^{3}$	0.1367E - 02	3.3	0.1280E - 02	3.9	0.1280E - 02	3.9
$64^{3}$	0.3711E - 03	3.7	0.3198E - 03	4.0	0.3198E - 03	4.0
rate	_	1.9	_	2.0	_	2.0

Table 4.4. Convergence of the fluid velocity components in the maximum norm (Example 4.1)

grid	$\ \varepsilon_{V^1}\ _c$	ratio	$\ \varepsilon_{V^2}\ _c$	ratio	$\ \varepsilon_{V^3}\ _c$	ratio
$8^{3}$	0.1867E + 00		0.1867E + 00		0.2818E + 00	
$16^{3}$	0.4256E - 01	4.4	0.4256E - 01	4.4	0.4992E - 01	5.6
$32^{3}$	0.1159E - 01	3.7	0.1159E - 01	3.7	0.1169E - 01	4.2
$64^{3}$	0.3802E - 02	3.0	0.3802E - 02	3.0	0.3236E - 02	3.6
rate	_	1.6	_	1.6	_	1.8

**Example 4.4.** In this example, we change the location of the layers from Example 4.3, which corresponds to  $\lambda_1 = 10^6$ ,  $\mu_1 = 10^6$ ,  $\varkappa_1 = 10^6$ ,  $\lambda_2 = 1$ ,  $\mu_2 = 1$ ,  $\varkappa_2 = 1$ . The respective convergence results are summarized in Tables 4.5 – 4.8. As in Example 4.3, the second order of convergence is observed for all unknowns.

Table 4.5. Convergence of u, v, w, p in the maximum norm (Example 4.2)

grid	$\ \varepsilon_u\ _c$	ratio	$\ \varepsilon_v\ _c$	ratio	$\ \varepsilon_w\ _c$	ratio	$\ \varepsilon_p\ _c$	ratio
$8^{3}$	0.1337E - 02	_	0.1337E - 02	_	0.2321E - 02	_	0.3858E - 02	
$16^{3}$	0.3637E - 03	3.7	0.3637E - 03	3.7	0.6153E - 03	3.8	0.9877E - 03	3.9
$32^{3}$	0.9189E - 04	4.0	0.9189E - 04	4.0	0.1563E - 03	3.9	0.2583E - 03	3.8
$64^{3}$	0.2308E - 04	4.0	0.2308E - 04	4.0	0.3942E - 04	4.0	0.6412E - 04	4.0
rate		2.0		2.0		2.0		2.0

Table 4.6. Convergence of the stress tensor components in the maximum norm (Example 4.2)

grid	$\ arepsilon_{S^{11}}\ _c$	ratio	$\ arepsilon_{S^{22}}\ _c$	ratio	$\ arepsilon_{S^{33}}\ _c$	ratio
$8^{3}$	0.1463E - 01	_	0.1463E - 01	_	0.1857E - 01	
$16^{3}$	0.5401E - 02	2.7	0.5401E - 02	2.7	0.4828E - 02	3.8
$32^{3}$	0.1598E - 02	3.4	0.1598E - 02	3.4	0.1224E - 02	3.9
$64^{3}$	0.4300E - 03	3.7	0.4300E - 03	3.7	0.3056E - 03	4.0
rate		1.9		1.9		2.0

Table 4.7. Convergence of the stress tensor components in the maximum norm (Example 4.2)

grid	$\ \varepsilon_{S^{12}}\ _c$	ratio	$\ \varepsilon_{S^{13}}\ _c$	ratio	$\ \varepsilon_{S^{23}}\ _c$	ratio
$8^{3}$	0.1256E - 01	_	0.1679E - 01	_	0.1679E - 01	_
$16^{3}$	0.4713E - 02	2.7	0.4708E - 02	3.6	0.4708E - 02	3.6
$32^{3}$	0.1405E - 02	3.4	0.1233E - 02	3.8	0.1233E - 02	3.8
$64^{3}$	0.3811E - 03	3.7	0.3133E - 03	3.9	0.3133E - 03	3.9
rate	_	1.9	_	2.0	_	2.0

Table 4.8. Convergence of the fluid velocity components in the maximum norm (Example 4.2)

grid	$\ \varepsilon_{V^1}\ _c$	ratio	$\ arepsilon_{V^2}\ _c$	ratio	$\ \varepsilon_{V^3}\ _c$	ratio
$8^{3}$	0.2021E + 00	_	0.2021E + 00	_	0.1743E + 00	_
$16^{3}$	0.4510E - 01	4.5	0.4510E - 01	4.5	0.4066E - 01	4.3
$32^{3}$	0.1207E - 01	3.7	0.1207E - 01	3.7	0.1074E - 01	3.8
$64^{3}$	0.3849E - 02	3.1	0.3849E - 02	3.1	0.3144E - 02	3.4
rate	_	1.6	_	1.6	_	1.8

**Example 4.5.** Consider a two-layer porous medium saturated with incompressible fluid (a = 0). A local load is applied to the upper surface of the medium to some square  $[x_1; x_2] \times [y_1; y_2]$ . The upper and lower surfaces of the medium are free to drain, and the lateral walls are rigid and impermeable. As a result of the applied load, the porous medium deforms and the fluid flows through the layers.

We solve this problem in the domain  $[0;1] \times [0;1] \times [0;1]$ . The following boundary conditions correspond to this situation:

 $\mathbf{S} \cdot \mathbf{n} = 0$ , p = 0 on the lower surface (z = 0),

 $\mathbf{u} = 0$ ,  $\mathbf{V} \cdot \mathbf{n} = 0$  on the lateral surfaces (x = 0 or x = 1 or y = 0 or y = 1),

 $\mathbf{S} \cdot \mathbf{n} = \sigma$ , p = 0 on the part of the upper surface  $(z = 1, (x, y) \in [x_1; x_2] \times [y_1; y_2])$ ,

 $\mathbf{S} \cdot \mathbf{n} = 0$ , p = 0 on the rest of the upper surface  $(z = 1, (x, y) \notin [x_1; x_2] \times [y_1; y_2])$ ,

where **n** is an outward normal to the considered surfaces and  $\sigma$  is the applied load.

The following parameters of the porous layers separated by the interface  $\xi = 0.499$  were considered - the lower layer:  $\lambda_1 = 10^4$ ,  $\mu_1 = 10^4$ ,  $\varkappa_1 = 10^{-1}$ ; the upper layer:  $\lambda_2 = 1$ ,  $\mu_2 = 1$ ,  $\varkappa_2 = 10^{-4}$ . As one can see from the parameters, the upper porous layer is softer, but less permeable than the lower one. The vertical local load of 5 is applied to the square  $[0.15; 0.25] \times [0.15; 0.25]$ , i.e.  $\sigma = (0,0,5)$ . The time interval is [0;1], and we use only one time step.

Some of the calculated physical characteristics of the process (in the corresponding cross-sections) are presented in Figs. 4.1-4.8. The calculations in this experiment were done on a grid  $32 \times 32 \times 32$ .

Figures 4.1 and 4.2 show the fluid pressure values in different cross-sections: the first cross-section crosses the local load and the second one does not. It is natural that the values of the fluid pressure are larger directly under the load than at some distance from it.

In Figures 4.3 and 4.4 vertical displacements are shown in the same cross-sections as the fluid pressure. The largest negative values for the vertical displacements are below the load (note that the z-axis is oriented upward). Note also that small positive vertical displacement appears at some distance from the load near the upper boundary.

It is well known that values of the stress tensor components are very important in many real problems. Figs. 4.5–4.8 show the tensor stress component  $S^{zz} = (\lambda + 2\mu) w_z + \lambda (u_x + v_y)$  in different vertical and horizontal cross-sections.

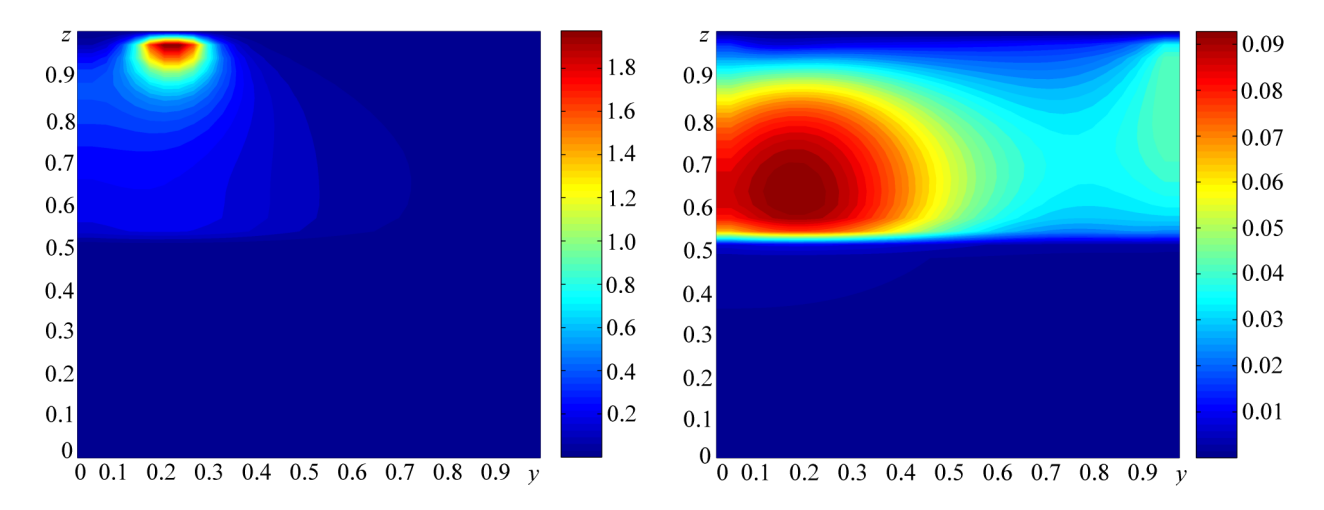


Fig. 4.1. Fluid pressure in the cross-section x = 0.1875 (Example 4.5)

Fig. 4.2. Fluid pressure in the cross-section x = 0.53125 (Example 4.5)

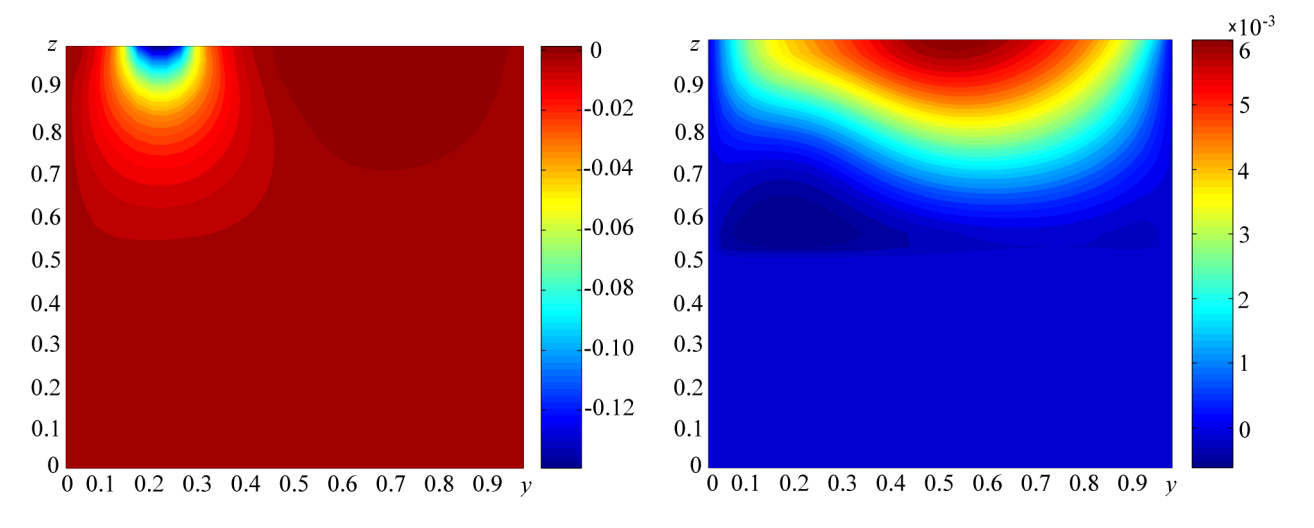


Fig. 4.3. Vertical displacement component in the cross-section x=0.1875 (Example 4.2)

Fig. 4.4. Vertical displacement component in the cross-section x = 0.53125 (Example 4.2)

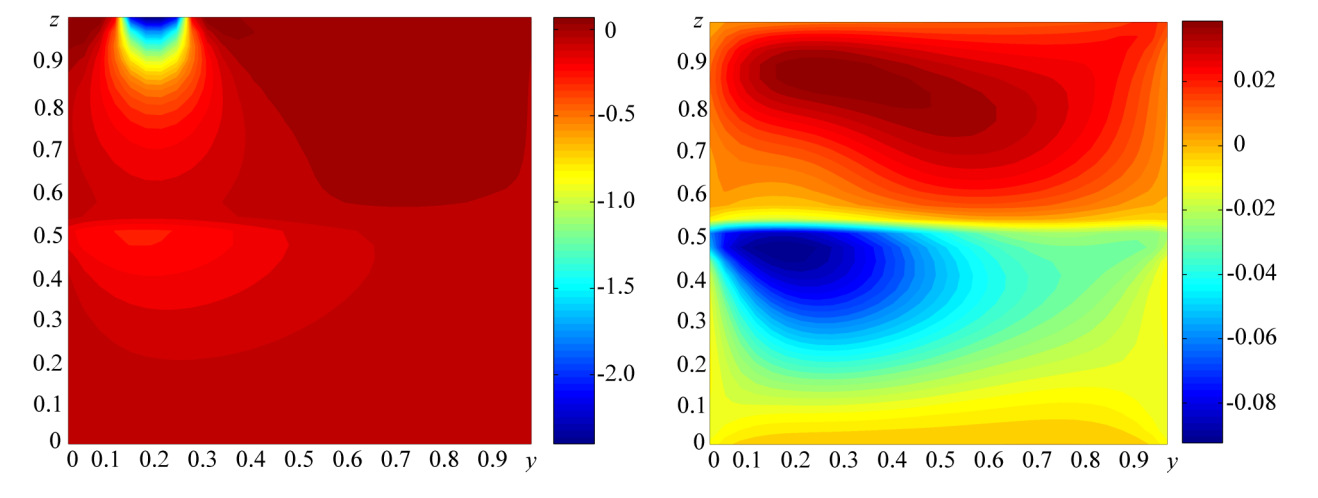


Fig. 4.5. Stress tensor component  $S^{zz}$  in the crosssection x=0.1875 (Example 4.5)

Fig. 4.6. Stress tensor component  $S^{zz}$  in the cross-section x=0.53125 (Example 4.5)

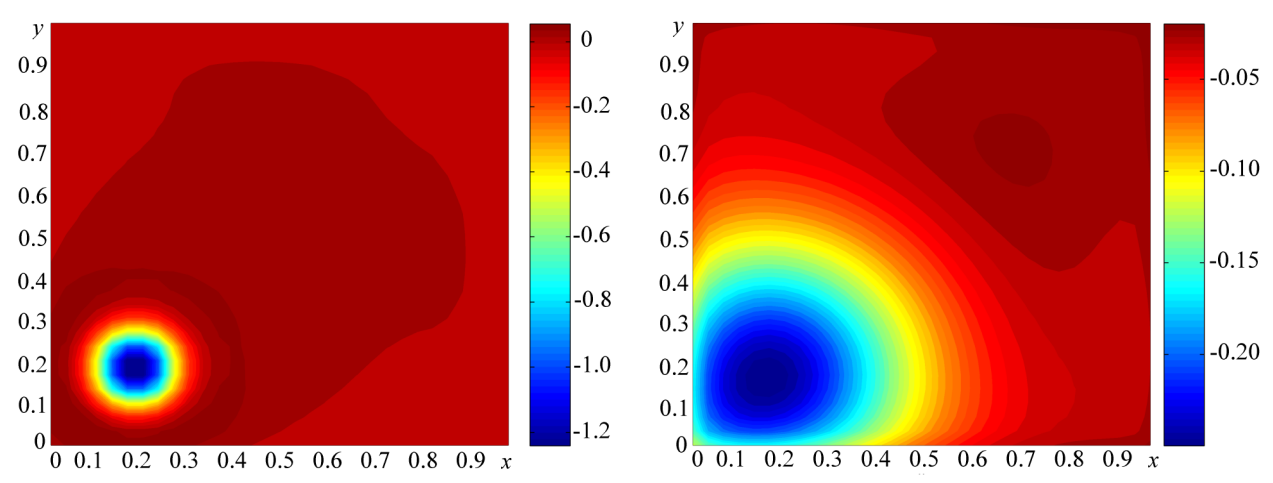


Fig. 4.7. Stress tensor component  $S^{zz}$  in the cross-section z=0.90625 (Example 4.5)

Fig. 4.8. Stress tensor component  $S^{zz}$  in the crosssection z=0.5 (Example 4.5)

## 5. Conclusions

In this paper, a finite volume discretization for the three-dimensional Biot poroelasticity system in a multilayer domain is proposed. This discretization specially takes into account for the discontinuity of the coefficients across the interface between subdomains with different physical properties. The numerical experiments, based on the proposed discretization, show second order convergence in the maximum norm of the primary and flux unknowns of the considered system. The method can also be used to model a certain physical process in a layered porous medium.

**Acknowledgments.** The author is in debt to Dr. Iliev and Dr. Lazarov for the valuable discussions. This work has been partially supported by the Kaiserslautern Excellence Cluster Dependable Adaptive Systems and Mathematical Modelling, and by EU under the INTAS project 03–50–4395.

#### References

- 1. J-L. Auriault and E. Sanchez-Palencia, Etude du comportement macroscopique d'un milieu poreux saturé déformable, Journal de Mécanique, 16 (1977), pp. 575–603.
  - 2. M. Biot, General theory of three dimensional consolidation, J. Appl. Phys., 12 (1941), pp. 155–169.
- 3. J.Bear and Y.Bachamat, Introduction to modelling of transport Phenomena in Porous Media, Kluwer Academic, Dordrecht, 1990.
- 4. J. R. Booker and J. C. Small, *Finite layer analysis of consolidation, part 1*, International Journal for Numerical and Analytical Methods in Geomechanics, **6** (1982), pp. 151–171.
- 5. Z. Cai, J. Douglas, and Jr. M. Park, Development and analysis of higher order finite volume methods over rectangles for elliptic equations, Adv. Comput. Math., 19 (2003), no. 1–3, pp. 3–33.
- 6. R. Ewing, O. Iliev, R. Lazarov, and A. Naumovich, On convergence of certain finite volume difference discretizations for 1-D poroelasticity interface problems Int. J. Num. Meth. PDEs, to appear.
- 7. R. Ewing, Zh. Li, T. Lin, and Ya. Lin, The immersed finite volume element methods for the elliptic interface problems, Math. Comput. Simul., **50** (1999), pp. 63–76.
- 8. R. Fedkiw, *The Ghost Fluid Method for Discontinuities and Interfaces*, Godunov Methods, Kluwer, New York, 2001, pp. 309-317.
- 9. F. J. Gaspar, F. J. Lisbona, and P. N. Vabischevich, A finite difference analysis of Biot's consolidation model, Appl. Numer. Math., 44 (2003), pp. 487–506.
- 10. B. Gurevich and M. Schoenberg *Interface conditions for Biot's equations of poroelasticity*, J. Acoust. Soc. Am., **105** (1999), no. (5).

- 11. O. Iliev, Finite volume discretizations for elliptic problems with discontinuous coefficients, Habilitation, University of Kaiserslautern, 2002.
- 12. R. W. Lewis and B. A. Schrefler, The finite element method in the static and dynamic deformation and consolidation of porous media, John Wiley, Chichester, 1998.
- 13. Zh. Li and K. Ito, Maximum principle preserving schemes for interface problems with discontinuous coefficients, SIAM J. Sci. Comput., 23 (2001), pp. 339–361.
- 14. K. Lipnikov, *Numerical methods for the Biot model in poroelasticity*, Ph.D. Thesis, Dept. of Mathematics, University of Houston, 2002.
- 15. M. A. Murad and A. F. D. Loula, On stability and convergence of finite element approximations of Biot's consolidation problem, Internat. J. Numer. Methods Engrg., 37 (1994), pp. 645–667.
- 16. A. Naumovich, O. Iliev, F. Gaspar, F. Lisbona, and P. Vabishchevich, On numerical solution of 1-D poroelasticity equations in a multilayered domain, Mathematical Modelling and Analysis, 10 (2005), no. 3, pp. 287–304.
- 17. A. A. Samarskii, *Theory of difference schemes*, Pure and Applied Mathematics, Marcel Dekker, New York, 2001.
  - 18. R. E. Showalter, Diffusion in poro-elastic media, J. Math. Anal. Appl., 251 (2000), pp. 310–340.
- 19. H. F. Wang, Theory of linear poroelasticity with application to geomechanics and hydrogeology, Princeton University Press, Princeton, 2000.
- 20. A. Wiegmann and K. Bube, The Explicit Jump Immersed Interface Method: Finite Difference Methods for PDE with piecewise smooth solutions, SIAM J. on Numerical Analysis, 37 (2000), pp. 827–862.
- 21. R. Wienands, F. J. Gaspar, F. J. Lisbona, and C. W. Oosterlee, An efficient multigrid solver based on the distributive smoothing for poroelasticity equations, Computing, 73 (2004), no. 2, pp. 99–119.